Monthly Weather Review
VOLUME 98, NUMBER 7
JULY 1970

UDC 551.553.11(764)

COASTAL AIR-CIRCULATION SYSTEM: OBSERVATIONS AND EMPIRICAL MODEL[1,2]

SHIH-ANG HSU
Coastal Studies Institute, Louisiana State University, Baton Rouge, La.

ABSTRACT

Three consecutive early summer studies on the upper Texas coast have produced data that afford a much clearer view of the land and sea breeze system than was previously held. Networks of surface observations, pibal and radiosonde ascents, and aircraft flights have produced observations that are integrated to give a synthesized model of the coastal air-circulation system as a function of space and time.

1. INTRODUCTION

The coastal air-circulation system as defined here consists of land and sea breezes (including bay and lake breezes) that are localized coastal circulations. The hypothesis to be examined is that the Texas coast sea breeze is a mesoscale four-dimensional moist circulation system in which the land and sea breezes can be described both in space and in time by the circulation theorem. This hypothesis is verified by observations.

An extensive sea breeze investigation has been underway at the University of Texas since 1965. Field experiments are designed in such a way that the observational results (samples) are most representative of the phenomenon studied. On the basis of observations obtained from 1965 through 1967, an empirical model in space and time of the Texas coast sea breeze system has been synthesized as shown briefly here. Some of the observational evidence collected will be presented to support the conclusions and the derived model. Methods of collecting data and some of the analysis procedures, in particular for upper air data, are summarized. For complete information about experiments and detailed analysis of data see Hsu (1969*a*).

2. EXPERIMENTS AND DATA EVALUATIONS

GENERAL FEATURES OF THE STUDY AREA

The study area (fig. 1) is the Port Arthur-Galveston section of the Texas coast on the Gulf of Mexico. This area includes 40 mi of straight coastline uninterrupted by bays and inlets. The study area is geologically a flat coastal plain underlain by Quaternary and Recent sediments that consist largely of sand, clay, and mud. The larger orographic features are two small terraces with elevations of about 30 and 20 ft above mean sea level; they are located near the center and at one end of the area, respectively (Big Hill and High Island in fig. 1). The 50-ft contour is near the northwestern part of the area near the town of Devers.

In the Gulf of Mexico, the 30-ft depth line is located about 3 n.mi. offshore. The average depth of both Galveston Bay and Sabine Lake is 6 ft. The mesoscale network stations (for example, Beach Station, abbreviated BCH, Stowell, STO, etc.) for the investigation of the Texas coast sea breeze are also shown in figure 1.

FIELD EXPERIMENTS

Various field experiments related to the present study were conducted during the period 1965 through 1967 in the study area:

1) Group experiments, that is, instrument comparison tests. The purpose of these experiments was to examine statistically a controlled data set for evidence of bias and random error.

2) Small- and medium-scale perpendicular-to-the-coast experiments. The purpose of these experiments was to study the horizontal gradients and their time variations in the study area.

3) Full-scale perpendicular-to-the-coast experiments. The mesoscale structure of the circulation system perpendicular to the coastline was investigated.

4) Parallel-to-the-coastline experiment. Study of the variations of the circulation system along the coastline was the object of this experiment.

5) Full-scale mesonet experiments. The purpose was to study the horizontal display of the main circulation

[1] Part of *Technical Report* No. 16 (Hsu 1969*a*).

[2] Paper presented at the American Geophysical Union-American Meteorological Society meeting on Apr. 24, 1969, at Washington, D.C.

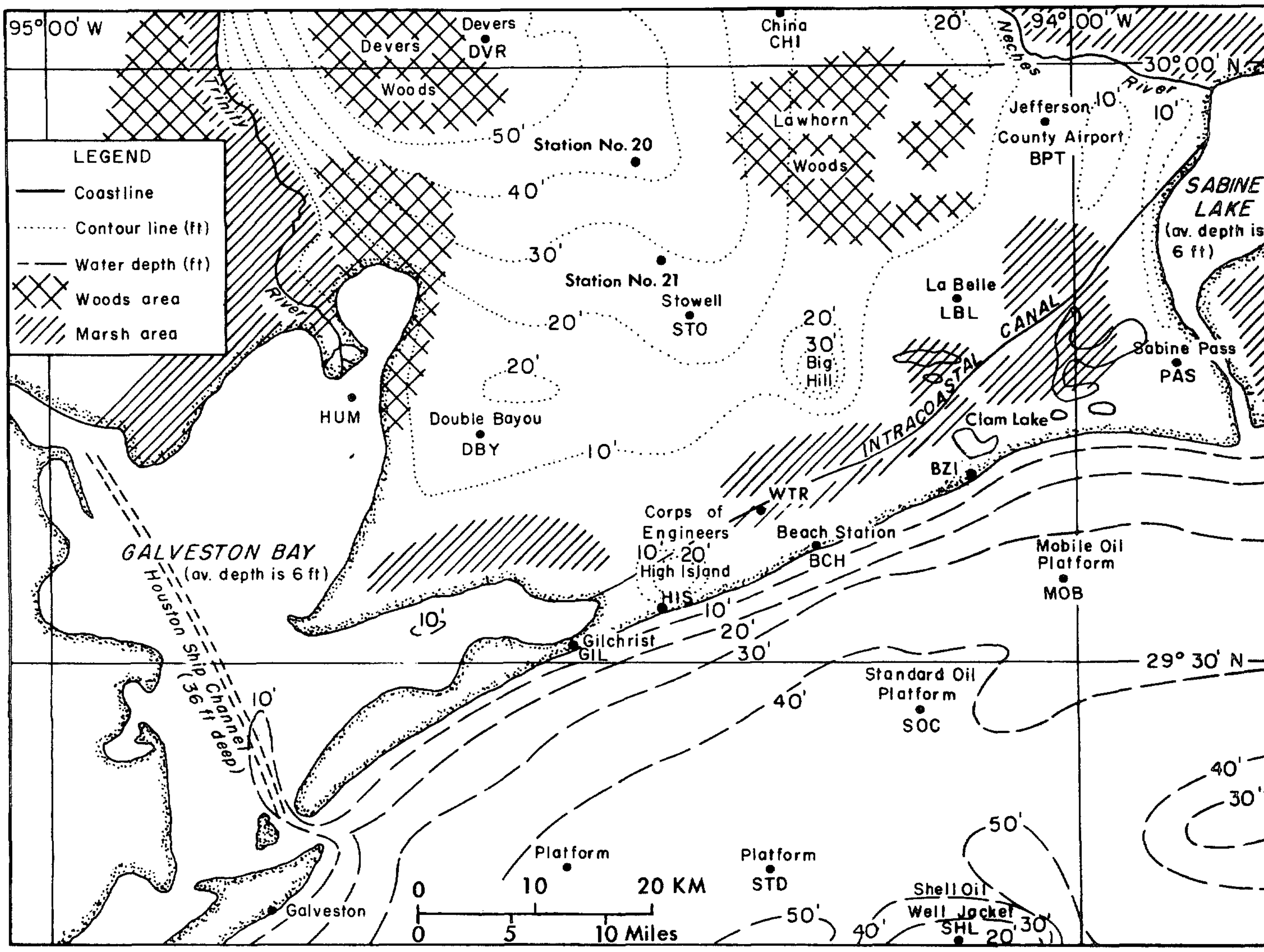

FIGURE 1.—General features of the study area.

features both in space and in time by means of the mesoscale network.

6) Twenty-four-hour intensive experiment. The land- and sea-breeze cycle was studied.

7) Sea-breeze convergence line experiment. Study of sea-breeze frontal characteristics was the object.

8) Water temperature measurements. These measurements were made in the bays, lakes, canals, and seashores in the study area.

DATA EVALUATION

The instrumentation used for the various experiments included, for collection of surface data, hygrothermograph, thermograph, microbarograph, and surface wind set; and, for upper air data, pilot balloon (theodolite set), radiosonde, and aircraft.

The parameters measured directly were temperature, pressure, relative humidity, and wind. These were observed both in space and in time from the surface up to 500 mb. A CDC 6600 computer was used to calculate additional parameters from pibal, radiosonde, and aircraft data. Included were dew point temperature; geopotential height; and onshore, offshore, and along-the-shore wind components for perpendicular- and parallel-to-the-coast vertical cross-sectional analyses.

Among the methods of collecting upper air data was an objective radiosonde data acquisition and reduction system developed by the author for the University of Texas Sea-Breeze Project. This method is summarized here; for more detail, see Hsu (1968). Briefly, that report describes a chain of events that begins with a mobile field system and ends with the reduced data in the digital computer. An objective, semiautomatic strip chart digitizer provides one of the unique aspects of the methodology.

The mobile field system consists of a van and trailer that transport and house equipment necessary for releasing and tracking the radiosonde and for making supporting surface observations. The operating procedure is convenient and simple. The objective radiosonde data-processing system consisted of a strip chart recorder, strip chart digitizer, and digital computer to provide the desired sample of data points for atmospheric pressure, temperature, relative humidity, geopotential height, and other desired meteorological parameters.

System evaluation shows that the error introduced by this technique to reduce the radiosonde data is small compared to that contributed by the radiosonde sensors themselves. Furthermore, this methodology is considerably more objective and less error-prone than the more pedestrian scheme normally employed. A completely automated system would, of course, be still better.

As for the statistical evaluation of sea-breeze data, only a brief summary will be given here. By means of analysis of variance technique, the relative bias between instruments from the group experiment data is known (Hsu 1967). The bias corrections for surface temperature and relative humidity for 1966 and 1967 were calculated from two group experiments, namely, the first, performed at the beginning of the field trip, and the last, performed at the end of the field trip. These group experiments were performed at Station BCH (fig. 1). For more detail, see Hsu (1967).

For the statistical evaluation of surface wind strip chart data, of aircraft data, and of radiosonde data gathered from the 1967 sea breeze field trip, see Eddy and Hsu (1968), Duchon (1968), and Hsu (1968), respectively.

3. MESOANALYSIS OF THE UPPER TEXAS COAST SURFACE TEMPERATURE AND UPPER WIND FIELDS

A study of the surface temperature field associated with the upper wind field is necessary to establish the concept that the sea breeze is a mesoscale thermally driven circulation. For the purpose of showing time variations in the horizontal patterns, 18 mesoscale surface temperature fields (3 hr apart) over the Texas coast sea-breeze study area for June 9 and 10, 1966, and for June 14 and 15, 1967, are presented in figures 2 and 3, respectively. The letters C and W in these mesoanalysis figures represent the areas of relative low and high temperatures, respectively. For reference, the relative humidity is also included for each station. The temperature and relative humidity indicated at each station, for example, BCH in figure 2a, should be read as 81.2°F and 79 percent, respectively. Note that these temperature and relative humidity values are all corrected according to the instrument-bias correction table calculated from our group experiments (Hsu 1969*a*).

From the mesocscale analysis of the upper Texas coast surface temperature field, based on the sea-breeze data gathered during the summer of 1966, Hsu (1967) suggests that there may be a cool pool about 15 mi inland over stations LBL, STO, and DBY between Sabine Lake and Galveston Bay (fig. 1). This cool pool may be caused by the cooling effects of the sea breeze during the day and enhanced by radiation during the night. This suggested cool pool also appears in the 1967 data analysis (fig. 3). Note that the construction of the isotherms near the coastal area is partially based on the fact that the main temperature gradient at night from land to sea is concentrated along the coast (Hsu 1967). This phenomenon gradually disappears after sunrise, as shown in figure 2e. Around noon, the temperature over land becomes higher than that over the ocean, as indicated in figure 2f. The situation of higher temperature over land is maintained until around the time of sunset except in the cool pool area (figs. 2g and 2h). At sunset, the diurnal cycle starts over again.

From the 24-hr intensive study (from 0900 CDT on June 14 to 0900 CDT on June 15, 1967), which will be investigated in section 4, figures 3a through 3j are obtained; they show the characteristics in the study area from 0600 CDT on June 14 to 0900 CDT on June 15, 1967 (3 hr apart). The convention in figure 3 is the same as that in figure 2. The temperature and relative humidity have also been corrected as mentioned previously. The bar at each station is the wind direction (the convention is shown on the figure). Wind speed is indicated at the end of the bar. The statistical evaluation for the wind data (Eddy and Hsu 1968) is given. The construction of isotherms is partially based on, in addition to the actual data, the mesonet experiment in the summer of 1966 (see, for example, fig. 2). Note that there were two major improvements in the observational network, which was redeployed in the 1967 field trip, over that of 1966 (fig. 2):

a) Denser perpendicular-to-the-coast mesonet, particularly in the vicinity of the coastal area (see stations BCH, WTR, WYT, RIC, and STO in fig. 3). The purpose of this kind of network deployment is to understand better the surface thermal patterns in space and time;

b) Two stations were added in the mesonet and set up near the southeastern portion near the coast in the study area, that is, stations CLK and SAB. The data obtained in 1966 at HIS, located in the southwestern section on the shore, showed that there is a relatively warmer region near this location (see, for example, fig. 2). However, since there is no station in the southeastern coastal area, it is the purpose of stations CLK and SAB to survey the thermal field in this region.

Figure 3a shows that at 0600 CDT there was a 12 mi hr^{-1} southerly wind at station SOC (about 12 mi offshore), but the wind decreased to 7.5 mi hr^{-1} at BCH (onshore), to 3.0 at WTR (about 3 mi inland), to 2.0 at WYT, to 0.5 at RIC, and to calm at STO (about 15 mi inland), JCT, and SOR. The wind direction shows that the wind veered with distance from the most northerly station, SOR (north wind), to JCT (NE.), STO (E.), RIC (SE.), WTR (SSE.), and BCH (S.) and SOC (S.). The facts that the wind speed continuously decreased and the direction backed from offshore to inland suggest a land breeze. However, because the general southerly flow, particularly the low-level jet produced by the Bermuda high-pressure system, was prevailing during this time (Hsu 1969*a*), this land breeze was suppressed to some extent. Other mesonet observations at the same time (that is, 0600 CDT),

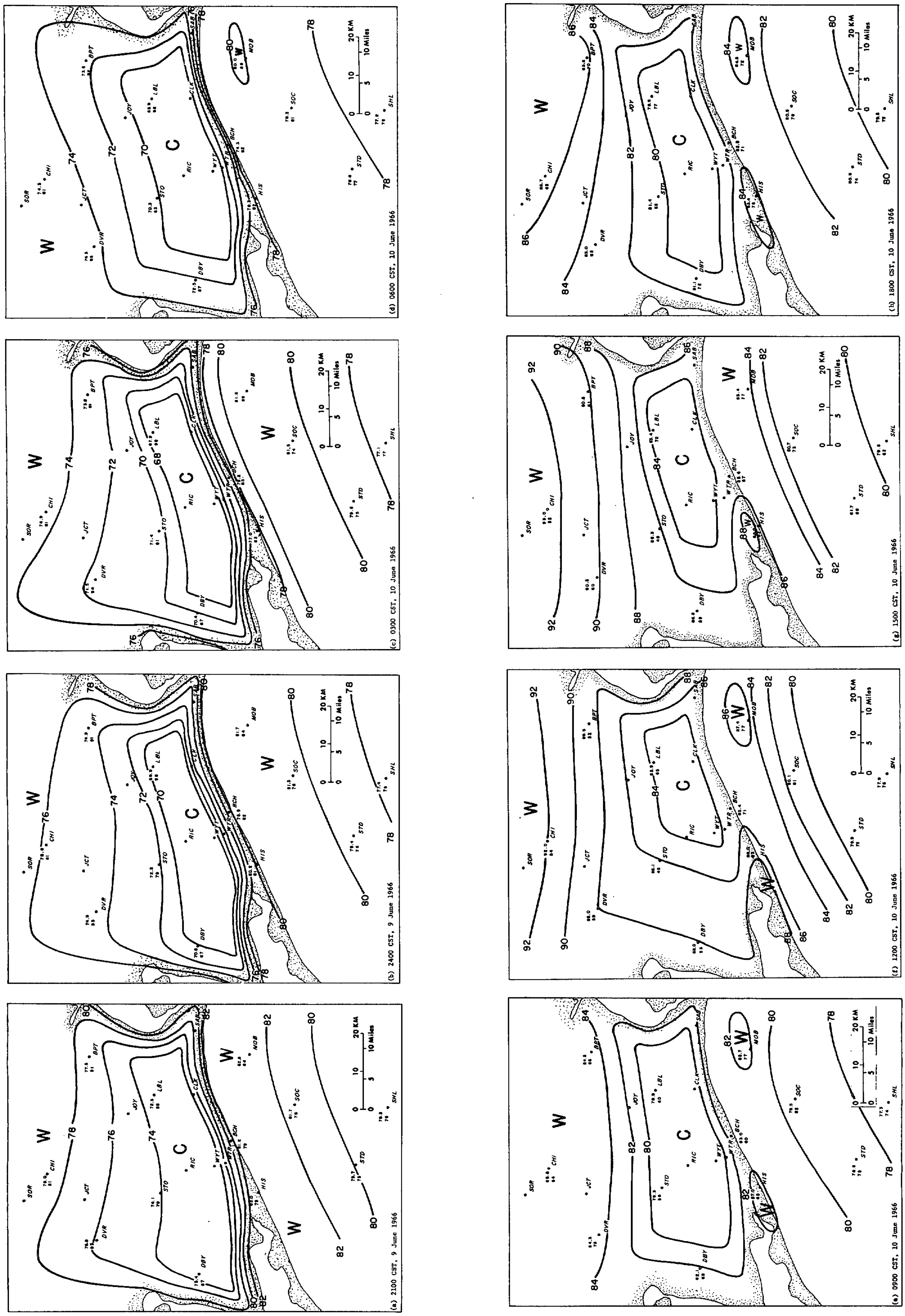

FIGURE 2.—Mesoanalysis of the upper Texas coast surface temperature field from 2100 CST on June 9 to 1800 CST on June 10, 1966.

shown in figure 3a, indicate that a line extends from stations BPT, JOY, and STO to DBY which separates this weak land breeze from the southerly flow.

The second feature shown in figure 3a is that the cool pool suggested by Hsu (1967) is clearly shown. Moreover, since the cool area extended to stations BPT, DBY, and WYT, further evidence is provided that the temperature gradient at late night and early morning from land to sea is concentrated along the coast.

Two relatively warm belts, namely, the northern warm belt, about 25 mi inland, and the southern warm belt, near the shallow gulf coastal area, suggested by Hsu (1967) are also shown in figure 3a.

Note that the air temperature over the ocean (station SOC) and the shallow gulf coastal area (BCH) is higher than that over land at 0600 CDT (fig. 3a). By 0900 CDT, the sun has risen and the temperature distribution has changed, as shown in figure 3b. Two warmer regions (the southeastern region, including stations CLK and SAB, and the southwestern region, including WTR, WYT, and HIS) appear at this time; this is different from the 1966 data (see, for example, fig. 2 and Hsu's (1967) figs. 11 through 26). The warming trend of the former region may be due to the effect of the nearby lakes, and that of the latter may be due to the nearby east Galveston Bay (fig. 1). Note that the former is about 3°F higher than the latter and that the latter is only about a half degree higher than station DBY, which is also located near Galveston Bay. Another warmer area at BPT may be due to the effect of petrochemical industries in the area.

Except in the warmer regions mentioned above, the temperature is more or less uniform in the study area (fig. 3b). The wind direction and speed also show that a general uniform southeasterly flow prevails at 0900 CDT. These facts indicate that any suggestion of a land breeze has died out by this time (fig. 3b). From noontime to evening, there is a relatively cooler region that has advanced from the coast to about 5 mi inland, as shown in figures 3c through 3e. The wind direction at SOC veers from E. to SSE. This may be due to the Coriolis effect. At 2100 CDT, the veering phenomenon (fig. 3f) for all stations is shown more clearly. At this time, the southeastern and southwestern warmer regions have disappeared, but the shallow Gulf Coast remains warmer than inland areas. The cooler center now is located near WYT, and the relatively cooler belt has started to form and extends from BPT, JOY, RIC, WYT to DBY. At midnight, the cooler center is located near STO, and the cooler pool and northern and southern warmer belt suggested by Hsu (1967) have been formed also. This situation is maintained until early morning of the next day, as shown in figures 3g through 3i.

Note that at 0600 CDT (fig. 3i) there is a belt ranging from BPT, JOY, and STO to DBY which separates the wind direction between NW. and NE. at and north of this belt from that between SW. and SE. to the south of this belt. This indicates that a land breeze is blowing at 0600 CDT, even though the wind speed is nearly calm. This weak land breeze, about 2 mi hr^{-1}, is shown more clearly at SOR, JCT, and BPT at 0900 CDT (fig. 3j). By this time, the belt that separates the land breeze and the general synoptic flow has retreated from the belt of BPT, JOY, STO, and DBY to that of BPT, JOY, and JCT. After sunrise, the cooler pool has disappeared and the warmer regions mentioned previously are showing up again (fig. 3j and compare to 3b).

From the preceding discussion of the surface characteristics in the study area from 0600 CDT on June 14 to 0900 CDT on June 15, 1967, it is shown that the land and sea beeezes may occur even during a southerly synoptic flow. It is interesting to note that stations MOB and HIS were not instrumented in 1967 but that the cool pool phenomenon was still clearly shown in figure 3 (compare with fig. 2 for 1966). Two additional such diurnal cycles for June 11, 1966, and June 14, 1966, have been studied by Hsu (1967).

In short, from figures 2 and 3 it is shown that the air temperature over the ocean is higher than that over land at night and in the early morning. Around noontime, the situation reverses except in the area affected by the sea breeze. This situation is maintained until after sunset; then the land becomes colder than the ocean until the next morning, when the diurnal cycle starts over again.

Figure 4 shows the height (z), time (t), and perpendicular-to-the-coast (x, with positive toward inland) variations of onshore and offshore wind components at stations SOC, about 12 mi offshore; BCH, near shore; and STO, approximately 15 mi inland. Notice that in this figure:

a) A positive value signifies an onshore wind component, and a negative, offshore;

b) The asterisk indicates the "theosonde" data, that is, the radiosonde balloon tracking by optical theodolite;

c) The surface temperature and relative humidity are indicated at each time of the pibal or theosonde observations;

d) The surface characteristics of the land- and sea-breeze front shown on the original hygrothermograph strip chart are also included in figure 4; and

e) The time sequence in this figure is from 1800 CST on June 9 to 1855 CST on June 10, 1966, a period which covers the time of figure 2.

The three-dimensional presentation shown in figure 4 indicates that the sea breeze blew at stations SOC, BCH, and STO from 1800 to 2400 CST on June 9, 1966. The return flow is also shown at each station. The average height of the wind reversal point or of the top of the sea breeze is approximately 1,900 ft. The average height of the top of the return flow is around 6,000 ft. After sunset and until the land breeze starts, both of these inflection points tend to lower with time until they reach the surface, at which juncture a reversal in the surface wind is observed. The maximum speed of this sea breeze occurs at 1800 CST. It ranges from 8 mi hr^{-1} at STO and SOC to 6 mi hr^{-1} at BCH; at 2100 CST, it is about 6 mi hr^{-1} at all stations; and at midnight, it decreases to about only 2 mi hr^{-1}. The maximum speed of the return flow is as follows: at 1800 CST, 11 mi hr^{-1} at STO and 10 mi hr^{-1} at both BCH and SOC; at 2100 CST, about 6 mi hr^{-1} at all stations; and at midnight, this return flow disappears since the sea breeze almost dies out at this time.

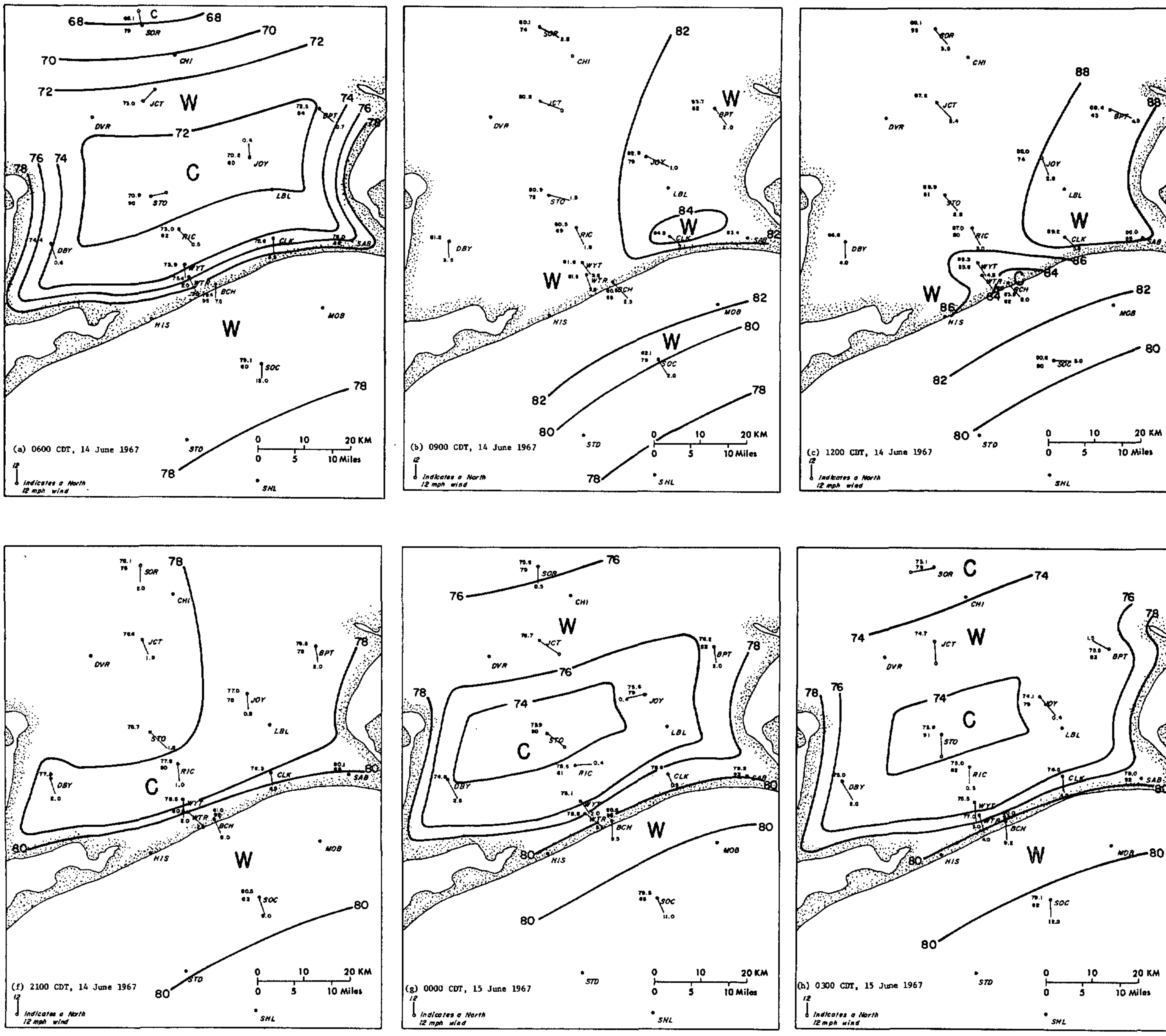

Note the S-shape of the onshore and offshore wind component structure. At 1800 CST, the upper portion of the S is bigger than the lower one; this indicates that a higher and stronger flow exists. At 2100 CST, the upper and lower portions of the S are the same, that is, the sea breeze and its return flow reach equilibrium stage. At midnight, the upper portion is gone and the lower one becomes much smaller, a fact which indicates that the return flow has diminished and the sea breeze is dying out.

The smaller diagram (A) shown in figure 4 indicates that the land-breeze front passed station BCH around midnight. The surface temperature drops approximately 4°F, and the relative humidity first decreases 2 percent and then increases about 2 percent. The pibal observations at BCH and SOC at 0300 CST indicate that the land breeze is almost twice as strong at BCH as at SOC. This suggests that the land breeze starts earlier near the coastal area than it does 12 mi offshore. The land breeze at this time has existed only for 2 or 3 hr and has not yet reached its full intensity; therefore, the return flow is small. At 0600 CST, a land breeze with a maximum speed of 10 mi hr^{-1} (offshore wind component) is observed at stations BCH and SOC, and one with a speed of about 12 mi hr^{-1} is seen at STO. The maximum speed of the return flow is about 9 mi hr^{-1} at SOC, 5 mi hr^{-1} at BCH, and 7 mi hr^{-1} at STO. The land breeze reaches its maximum speed (about 15 mi hr^{-1}) at 0625 CST at BCH, as shown in the figure. At 0900 CST, the maximum offshore component is about 8 mi hr^{-1} at SOC and BCH and 6 mi hr^{-1} at STO. By this time, the return flow becomes deeper and reaches the reversed S

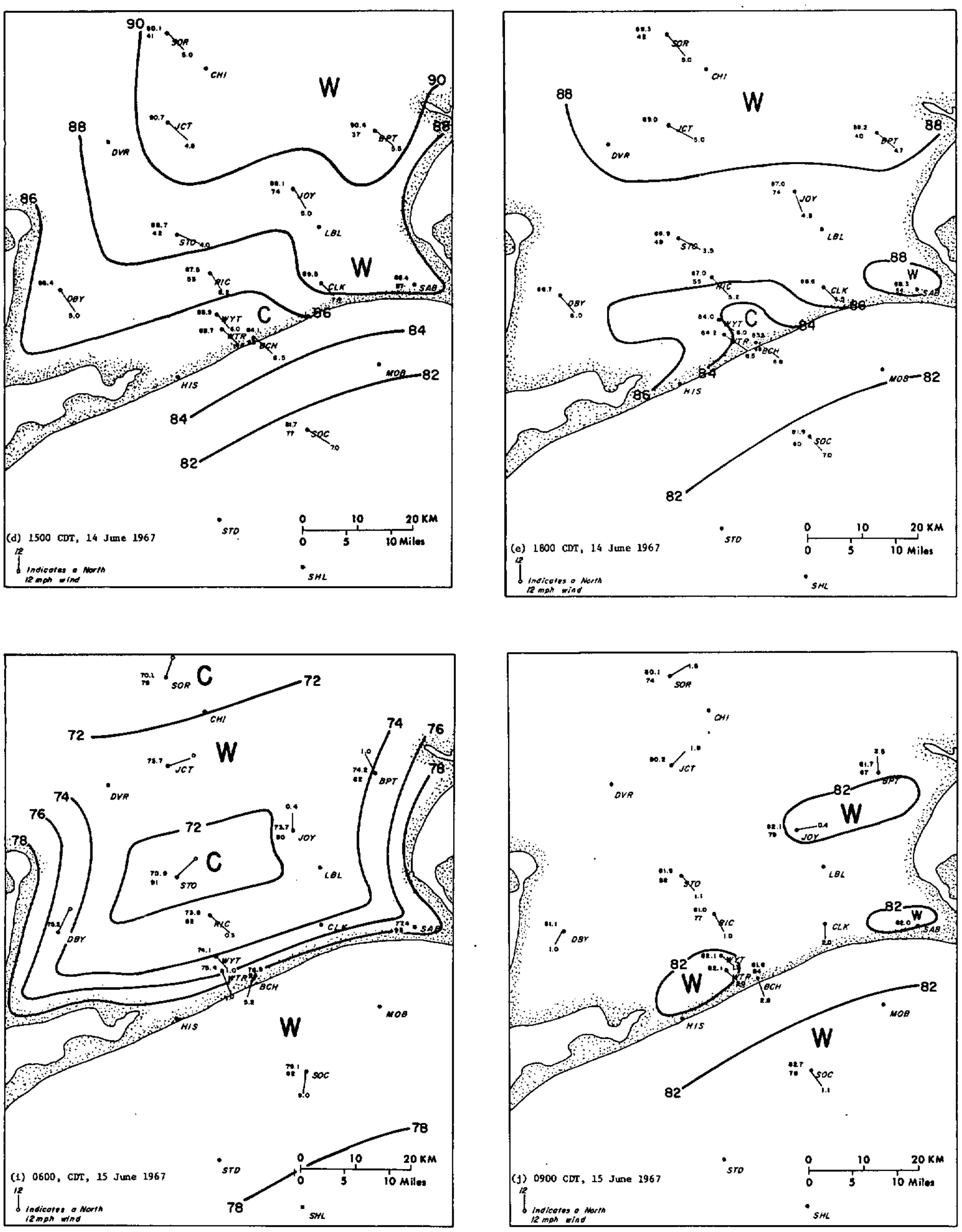

FIGURE 3.—Mesoanalysis of the upper Texas coast surface temperature field from 0600 CDT on June 14 to 0900 CDT on June 15, 1967.

shape. The average height of this land breeze is about the same as that of the sea breeze, that is, approximately 1,900 ft. The height of the top of the return flow increases with time, varying from 3,300 ft at 0300 CST to 7,000 ft at 0900 CST.

Near 1100 CST on June 10, 1966, the sea-breeze front was passing over station BCH, as shown in the small diagram (B) in figure 4. The surface temperature drops approximately 4°F, and the relative humidity first decreases 7 percent, then increases 13 percent. At 1200 CST, the sea breeze already has started blowing at stations BCH and SOC, while the land breeze is still prevailing at STO, even though its speed is only about 1 mi hr^{-1}. Note that the maximum speed of the sea breeze at BCH at this time is approximately four times higher than that at SOC, while farther inland STO still has a land breeze. Thus at 1200 CST, we see lines of offshore low-level divergence and onshore low-level convergence. Onshore divergence above 1,000 ft is also seen at this time. This evidence strongly supports the concept that the sea breeze starts earlier near the coastal area than at either farther inland or offshore. Around 1400 CST, the sea-breeze front was passing over station STO. The temperature dropped about 4°F, and the relative humidity first decreased 11 percent and then increased 14 percent, as shown in figure 4C. Further evidence on the effect of land- and sea-breeze fronts on the Gulf Coast is given elsewhere (Hsu 1969*b*).

At 1500 CST, the sea breeze is inland from STO, and the maximum speed at SOC has increased from 2 to 9

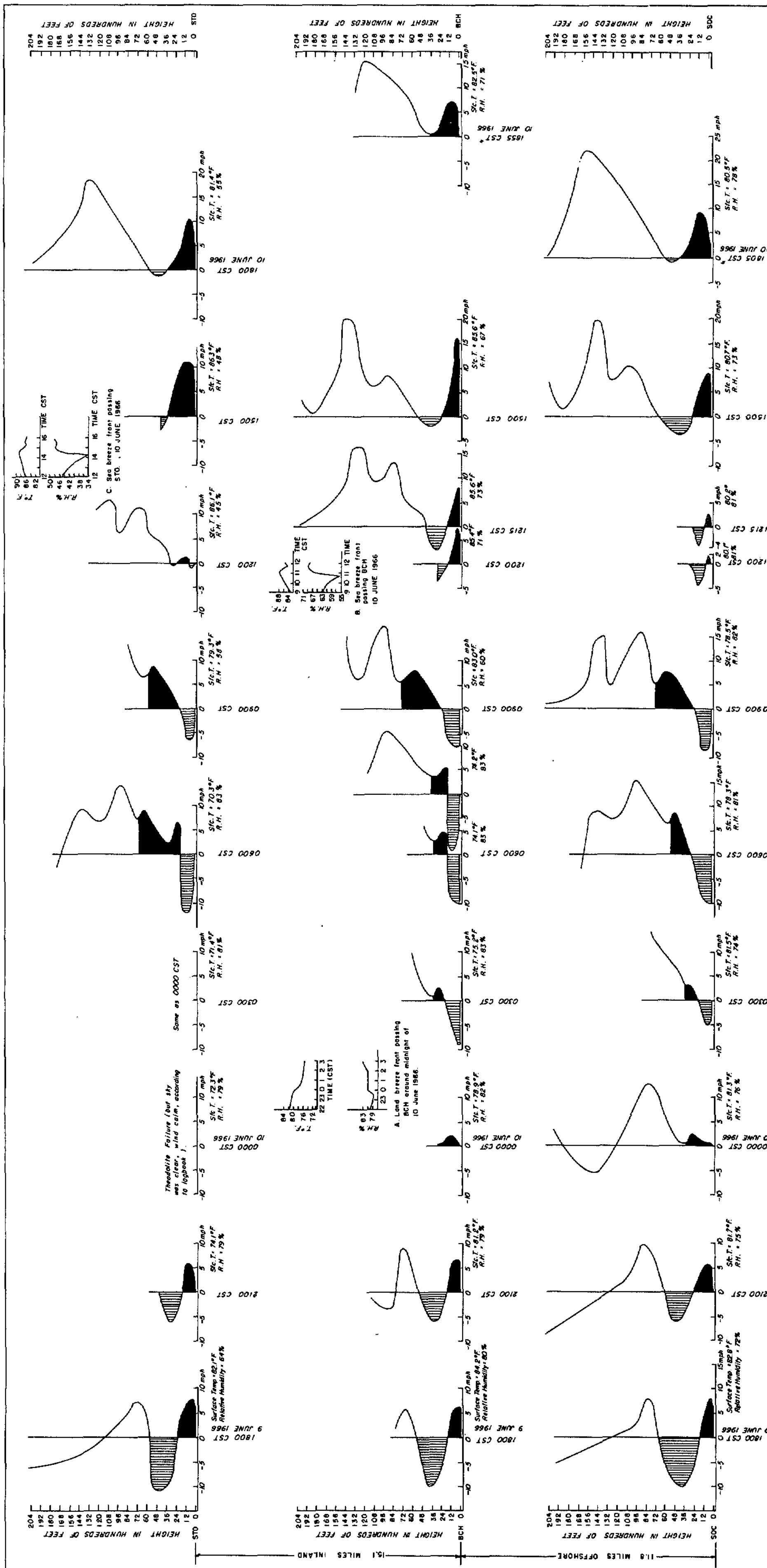

FIGURE 4.—The x-z-t three-dimensional variations of land and sea breezes from 1800 CST on June 9 to 1855 CST on June 10, 1966, at stations SOC, BCH, and STO, which are perpendicular to the coastline.

mi hr^{-1}. The structure shown at BCH at this time shows not only greater speed but shallower depth than that at STO and SOC. This may be due to the subsidence warming of the return flow near the coastal area, which will be discussed in the next section. After 1500 CST, the sea breeze continues to blow until the next cycle starts. The height of this sea breeze varies from 600 ft at 1200 CST to 3,900 ft at 1805 CST at SOC, from 1,500 ft at 1200 CST to approximately 3,600 ft at 1855 CST at BCH, and from a land breeze at 1200 CST to about 3,600 ft at 1800 CST at STO. The height of the top of the return flow also varies with time. On the average, however, it ranges from 2,700 ft at 1200 CST to approximately 6,000 ft at 1500 and 1800 CST. The speed of the return flow is also shown in the figure.

The foregoing discussion of the surface temperature fields (figs. 2 and 3) and the land- and sea-breeze winds (fig. 4) gives strong indication that the sea breeze is a mesoscale thermally driven circulation. Further evidence is given in Hsu (1969*a*).

4. LAND-BREEZE AND SEA-BREEZE SYSTEMS GOVERNED BY THE CIRCULATION THEOREM

The land- and sea-breeze effect across the Texas coast may be explained by means of the solenoid field. Eight solenoid fields (3 hr apart) perpendicular to the coast for the 24-hr observational period have been constructed and are shown in figures 5a through 5h. The data are from the three manned stations, namely, SOC (approximately 18 km offshore), BCH (near the gulf shore), and STO (approximately 24 km inland). These charts are plotted according to the following:

a) From the theosonde observation, we have every minute's actual position of the radiosonde balloon, including height and horizontal displacement. These data are first plotted in the chart. Since the sea breeze is a mesoscale phenomenon and the balloon may sometimes drift to a position between two mesonet stations, the actual position of the radiosonde balloon must be plotted; that is, the horizontal displacement of balloon position cannot be neglected.

b) The corresponding data (also every minute time interval) of geopotential height, atmospheric pressure, dry-bulb temperature, and dewpoint temperature are entered at the corresponding position, from a).

c) Linear interpolation is made between successive data points for each parameter, for example, every 2°C for temperature.

d) Isopleths of pressure, temperature, and dewpoint temperature are constructed as shown in figures 5a through 5h.

Figures 5a through 5c show the vertical cross sections through the atmosphere in the upper Texas coast from 1200 to 1800 CDT on June 14, 1967. Since the land becomes warmer than the sea during the day, the surfaces of constant temperature slope upward from sea to land below 500 m on June 14, 1967. Because the observed isobaric surfaces are more nearly horizontal, the two sets of lines intersect to form a solenoid field in the vertical plane. The rate of change of circulation around a vertical circuit half over land and half over water will be negative—that is, clockwise. If the initial circulation is zero or nearly so, the subsequent circulation will be such as to bring cool air from the sea toward the warm land at low level—in the present case, below approximately 500 m. At upper levels, one would expect a return flow of warm air from the land to the sea. This is shown at elevations between 1000 and 1500 m at 1200 CDT, between 500 and 4000 m at 1500 CDT, and between 500 and 1500 m at 1800 CDT. This assumption is supported by the dewpoint temperature, since the relatively drier dewpoint temperatures near the coastal area (station BCH) show that there exists a subsidence phenomenon, particularly at 1500 CDT, which is near the fully developed sea breeze, as shown in figure 6. This feature could occur if drier air from aloft were advected into the region of horizontal divergence at the inland boundary of the return flow. This phenomenon has also been observed from a fully developed lake breeze on the eastern shore of Lake Michigan (Moroz 1967, fig. 5). This subsidence phenomenon near the coastal area is further supported by a color photograph taken at SOC that indicated a few scattered weak cumulus clouds near SOC separated from the convergence line (a line of Cu) onshore by a large clear area.

At night, the land cools by radiation while the sea surface maintains a more uniform temperature because of the enormous reserve of heat in the sea. Thus, the isotherms will have the opposite slope from those in figures 5a through 5c, and a circulation of opposite sense will be developed. This is shown below 500 m in figures 5d through 5g. The radiational cooling effect is shown clearly at STO, as indicated in figures 5e, 5f, and 5g. Because of the inversion shown in figures 5f and 5g, the air at night is more stable. Therefore, the dewpoint temperatures below 500 m are more uniformly distributed over the study area.

At 0900 CDT (fig. 5h), the temperature is nearly uniform near the surface; but at higher elevation, say between 1000 and 975 mb, more solenoids exist, so that the sea breeze starts above the surface first. Moreover, from the aircraft data gathered during the 24-hr study period, the temperature traces at 1,000 ft show that a baroclinity develops over land and inland from station BCH in early morning. As the day progresses, the baroclinic field extends both landward and seaward until sunset. Detailed analysis is given in Hsu (1969*a*).

An attempt to incorporate the radiosonde data with the aircraft data is given to illustrate further that the Texas coast sea breeze is driven by the solenoid field. Figure 6 shows the full-scale perpendicular-to-the-coast cross section at 1500 CDT on June 14, 1967. This is close to the time of the maximum temperature difference between land and water. Before figure 6 is explained, a few procedures used to construct this figure should be mentioned:

a) A comparative study of the radiosonde and aircraft data was made from the balloon-chasing experiments at STO and the 24-hr experiment at SOC, BCH, and STO. The aircraft data used in this study were restricted to those instances in which, at a particular level, the separation in time between aircraft and radiosonde was

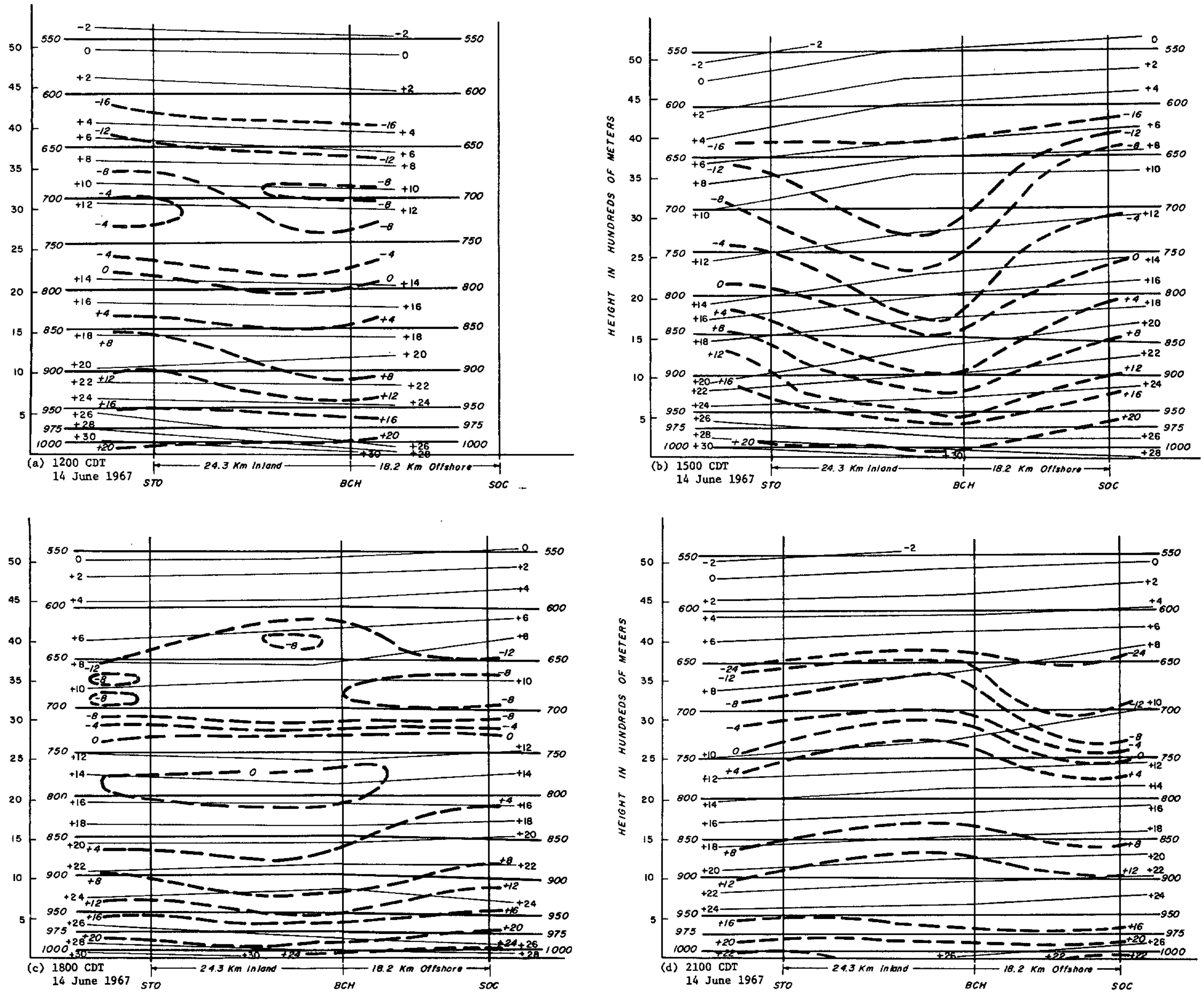

FIGURE 5.—Pressure (thick solid lines), dry bulb (thin solid lines), and dew point (heavy dashed lines) temperature structure in in the vertical from (a)–(d) 1200 to 2100 CDT on June 14, 1967, and (e)–(h) 2400 CDT on June 14 to 0900 CDT on June 15, 1967.

less than ± 15 min. The aircraft data are then corrected according to these experiments.

b) Since the actual height of the pressure surface of the aircraft is not precisely known and the observed pressure surfaces are nearly horizontal, as shown in figures 5a through 5h, the isobaric surfaces from the three radiosonde stations, STO, BCH, and SOC, must be extrapolated to SHL (seaward) and to Devers and Votaw (landward) as shown in figure 6. Note that the stations shown in figure 6 are nearly perpendicular to the coastline.

c) The corrected aircraft data are entered at the proper pressure surfaces. Since the aircraft sampled at most only about four levels above each station, linear intrapolation between two succeeding levels is necessary.

d) The isotherms are contructed as shown in figure 6.

Figure 6 shows that at 1500 CDT on June 14, 1967, the baroclinic field developed approximately from stations SHL (40 km offshore) to DVR (57 km inland), and the barotropic field was observed from DVR and, farther inland (approximately 101 km), to station VOT. Moreover, in general the direct solenoidal circulation is from sea to land below approximately 900 mb and from land to sea between 900 and 700 mb. Note that two cells of solenoids appear between 900 and 850 mb, and still higher, between 800 and 700 mb, over STO. These may be due to the low-level convergence associated with the upper level divergence phenomenon shown in the next section. From the upper wind observations, it has been shown (Hsu 1969*a*) that the sea-breeze effect extends to about 9,000 ft (approximately 700 mb, fig. 6), indicating a deeper

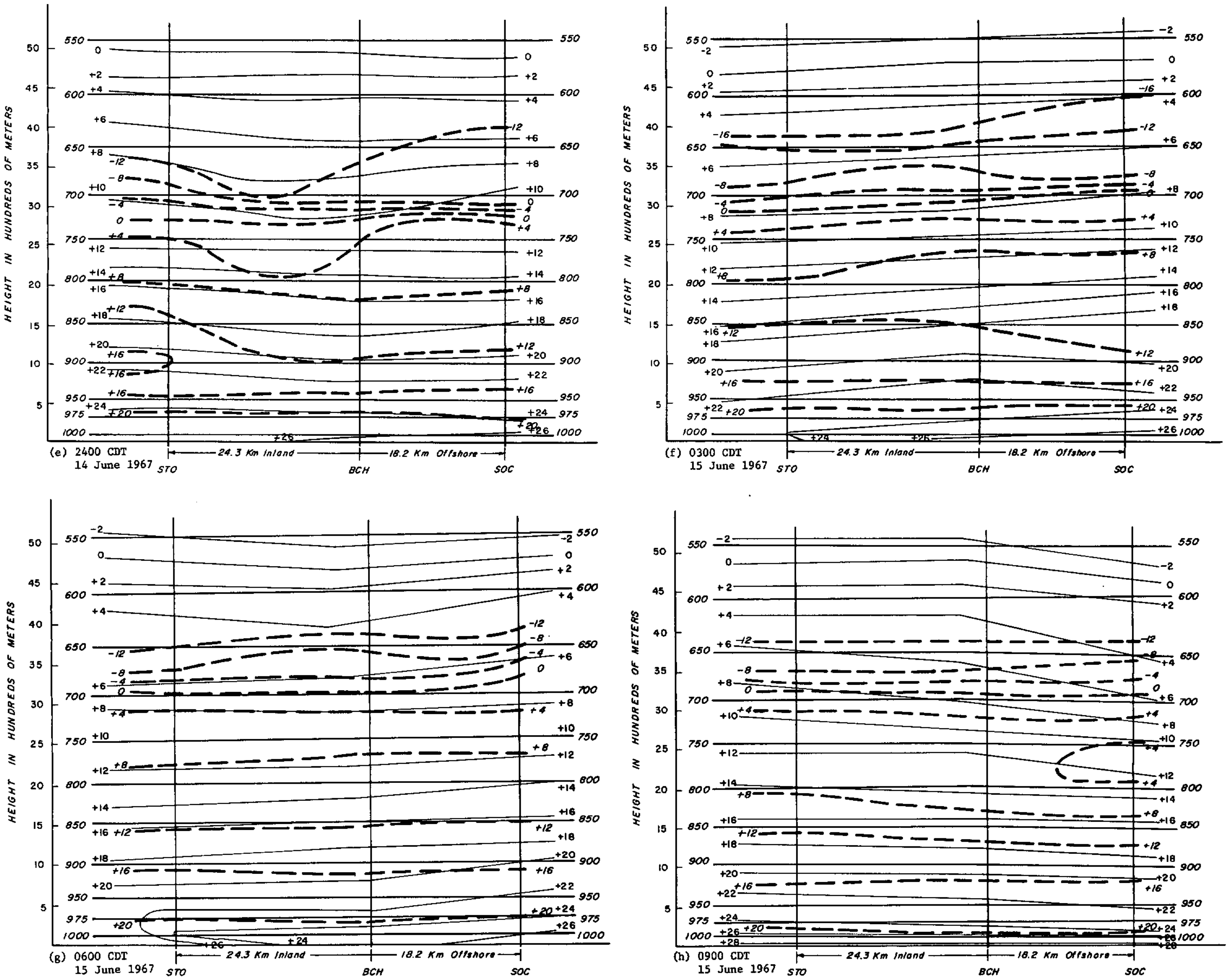

FIGURE 5.—Concluded.

circulation pattern at this time. Furthermore, the weather observation made at STO at 1500 CDT on June 14, 1967, shows that there is a line of cumulus and towering cumulus clouds ranging from the northwest to the distant north of STO. (See the "Sea Breeze Logbooks" for STO by the Atmospheric Science Group 1965–1967.) This indicates that there is a line of convergence at this time. The convergence line will be discussed in a later section. On the basis of these three observational results, namely, baroclinic field, wind field, and cloud observation, the mean speed of the sea-breeze circulation perpendicular to the Texas coast can be estimated, as follows:

The sea-breeze circulation to be considered in figure 6 requires a temperature difference between the air over land ($\overline{T}_a$) and that over water ($\overline{T}_b$), that is, $\overline{T}_a-\overline{T}_b$. According to the customary form of Bjerknes's circulation theorem (see, for example, Hess 1959), if friction is neglected, it is found that the intensity of the sea breeze will increase until $\overline{T}_a-\overline{T}_b$ changes from positive to negative values. According to Haurwitz (1947), however, owing to the effect of friction, the maximum sea-breeze intensity occurs not when $\overline{T}_a-\overline{T}_b$ has decreased to zero but earlier, while the land is still warmer than the sea. The reason for this is that a specific, positive temperature difference is required just to overcome the frictional force. Thus, a balance is possible between the increase in circulation caused by the mass distribution and the decrease caused by retarding friction; consequently, steady wind may be calculated from our actual observation, as shown in figure 6.

Taking friction into account, consider a sea-breeze circulation that takes place in a vertical x, z plane, with the x-axis perpendicular to the coastline, as shown in figure 6. The path of integration chosen is as indicated by

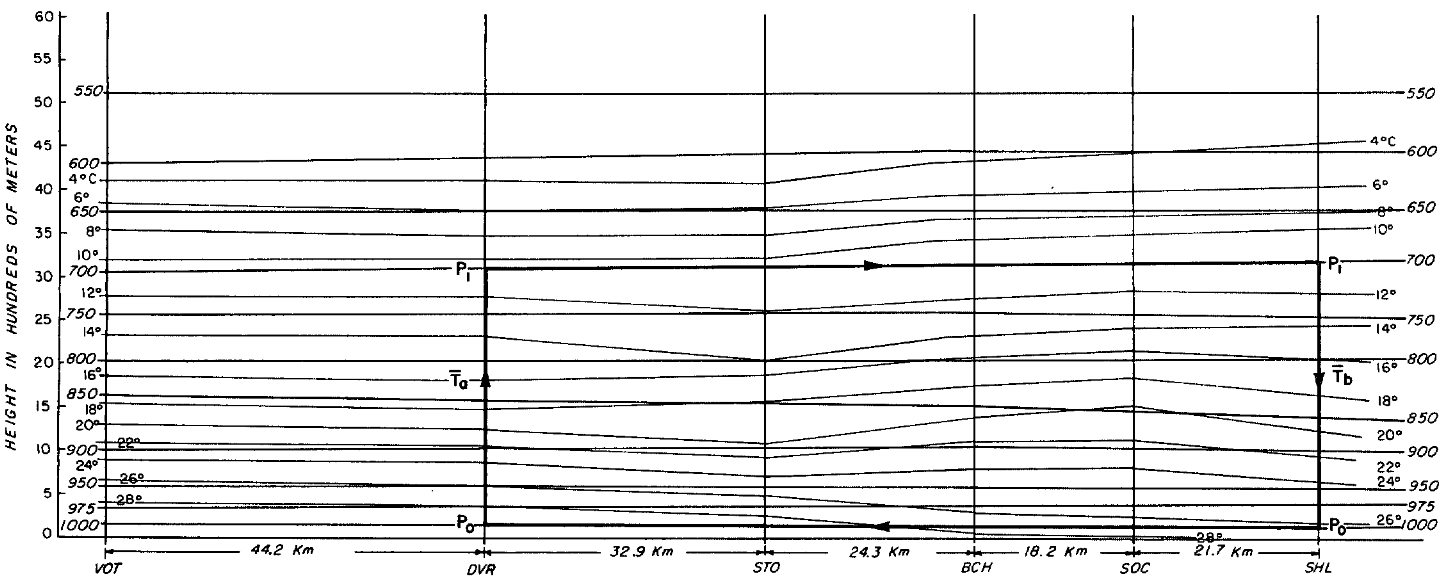

FIGURE 6.—Baroclinic and barotropic fields on the upper Texas coast at 1500 CDT on June 14, 1967. Thick lines are isobaric surfaces; thin lines are isotherms; and the heavy line is the path of integration for the sea breeze circulation system.

the heavy solid line, which is based on the observational results mentioned above. The frictional force is assumed to be opposite to and proportional to the wind velocity. Thus, the equations of motion can be written as

$$\frac{du}{dt}+ku=-\frac{1}{\rho}\frac{\partial p}{\partial x} \tag{1}$$

and

$$\frac{dw}{dt}+kw=-\frac{1}{\rho}\frac{\partial p}{\partial z}-g \tag{2}$$

where u and w are the velocity components in the x- and z-directions, respectively, p is the pressure, ρ is the density, g is the acceleration of gravity, and k is a constant that expresses the intensity of the frictional force. The resulting circulation may be expressed as

$$C=\oint(udx+wdz)=L\overline{V} \tag{3}$$

where L is the length of the path of integration and $\overline{V}$ is the mean speed of the sea-breeze circulation along the the path of integration.

By multiplying equation (1) by dx, equation (2) by dz, adding, and integrating around the closed path, the rate of change of the circulation C is found to be

$$\frac{dC}{dt}=\oint\left(\frac{du}{dt}\,dx+\frac{dw}{dt}\,dz\right)=-\oint\frac{dp}{\rho}-\oint gdz-kC$$

$$=R(\overline{T}_a-\overline{T}_b)\ln\frac{P_0}{P_1}-kC \tag{4}$$

where $R(=2.87\times10^6$ ergs/gm/°K) is the gas constant for air. Then from equations (3) and (4), one gets

$$\frac{d\overline{V}}{dt}+k\overline{V}=(\overline{T}_a-\overline{T}_b)\,\frac{R}{L}\ln\frac{P_0}{P_1}=K(\overline{T}_a-\overline{T}_b). \tag{5}$$

The quantity $K=(R/L)\ln(P_0/P_1)$ is constant, since for a fixed path of integration P_0 and P_1 are constant.

In the sea-breeze problem, $\overline{T}_a-\overline{T}_b$ is assumed to be a periodic function of time on the basis of observational results from 1966 sea-breeze data gathered at SHL and DVR. Using Fourier analysis, Hsu (1967) found that a simple harmonic function fits the data of $\overline{T}_a-\overline{T}_b$ quite well over the entire 24-hr period. In fact, one can explain 88 percent of the variance with wave number 1. Thus,

$$K(\overline{T}_a-\overline{T}_b)=A\cos\Omega t \tag{6}$$

where $\Omega(=7.29\times10^{-5}\text{ sec}^{-1})$ is the angular velocity of the earth. Equation (6) implies that the time is reckoned from the instant when $\overline{T}_a-\overline{T}_b$ reaches its maximum, that is, when $t=0$, then $\overline{T}_a-\overline{T}_b$ has its maximum value. Putting equation (6) into (5) and integrating, we find the solution of the resulting differential equation to be

$$\overline{V}=\text{const }e^{-kt}+A(k^2+\Omega^2)^{-1}(\Omega\sin\Omega t+k\cos\Omega t). \tag{7}$$

The arbitrary constant in equation (7) can be assumed to be zero because, in the absence of a temperature difference ($A=0$), the wind should be zero. Hence, equation (7) becomes

$$\overline{V}=A(k^2+\Omega^2)^{-1}(\Omega\sin\Omega t+k\cos\Omega t). \tag{8}$$

In the Texas coast sea-breeze area, the path of integration may be determined from the observational data, as shown in figure 6, that is, $P_0=1000$ mb, $P_1=700$ mb, $L=200$ km, and $\overline{T}_a-\overline{T}_b=5$°C. This is slightly larger than the circulation area considered by Fisher (1960). Substituting these values into equations (5) and (6), one finds that

$$K=0.05\text{ cm sec}^{-2}\text{ deg}^{-1}$$

and

$$A=0.25\text{ cm sec}^{-2}.$$

According to observations (Hsu 1967, fig. 32), $\overline{T}_a-\overline{T}_b$ reaches its maximum around 1200 CST (that is, $t=0$ at 1200 CST). If we assume the friction $k=2\times10^{-5}$ sec^{-1} in the coastal area, as suggested by Haurwitz (1947), and substitute $t=0$ into equation (8), we find that the mean speed of the sea-breeze circulation ($\overline{V}$) perpendicular to the Texas coast is 8.8 m sec^{-1}. This is in agreement with the observations (see, for example, fig. 4 around 1500 CST).

5. A COMPLETE LIFE CYCLE OF THE TEXAS COAST SEA BREEZE

One of the many important experiments performed in the Sea Breeze Project during the summer of 1966 was the 28-hr experiment from 0400 CST on June 14 to 0600 CST on June 15, 1966. During this period, the three main stations (SOC, BCH, and STO) released pibals every hour, a radiosonde replacing the pibal every third hour. One mobile pibal unit was also in operation. From these pibal and theosonde observations, the upper air wind field can be analyzed and consequently a complete life cycle of the Texas coast sea breeze may be studied.

From synoptic analyses (Hsu 1969*a*), it has been shown that the prevailing synoptic flow was northeasterly, or approximately parallel to the coast, and high pressure was centered over the land during the 24-hr study period. However, this synoptic flow was rather weak from the surface to 500 mb. Thus, the synoptic flow on this date has no great effect on the land- and sea-breeze systems in the upper Texas Gulf Coast, as is also shown on daily weather maps by ESSA. In other words, if one analyzes the upper air wind data from pibal and theosonde observations, the land- and sea-breeze cycle should show up. This is done, and the results are shown in figures 7a through 7c.

Six upper air wind-observing stations were operated during the 28-hr experiment, namely, SOC, BCH, WTR, STO, and stations 21 and 20; they ranged from 12 mi offshore to approximately 24 mi inland. Among these six stations, WTR, station 20, and station 21 were operated by the mobile pibal unit. These stations were more or less perpendicular to the coast (fig. 1). The relative distance between two succeeding stations is shown on the left side in figure 7a. Other conventions in this figure are the same as in figure 4.

Several interesting features may be seen from figures 7a through 7c:

a) Between 0400 and 0500 CST on June 14, 1966, the sea breeze is still prevailing offshore, even though it is rather weak (only about 2 mi hr^{-1} at most), while the land breeze already has started to blow over land. Furthermore, the land breeze is stronger below 1,000 ft near the coastal area than it is farther inland. It has already been shown that the land breeze starts earlier near the coastal area between shore and approximately 4 mi inland. Thus, the land breeze starts earlier and stronger in the nearshore area than both farther inland and offshore.

b) The average speed and height of this land breeze observed by all stations on this date are approximately 5 mi hr^{-1} and 2,200 ft, respectively. Of course, speed and height are subject to time variations, as discussed previously. The absolute return flow of this land breeze (except at 1000 CST at STO) may be masked by the offshore component of the synoptic flow. However, the relative return flow is still shown: see, for example, STO, WTR, BCH, and SOC near 0800 CST.

c) Near 1000 CST, the land breeze becomes weaker at BCH than at STO and SOC. Near 1100 CST, the sea breeze is observed at all stations. However, the sea breeze extends to a higher elevation at BCH than at STO and SOC. The deeper and stronger sea breeze at BCH is shown clearly near 1200 CST. Comparison of this feature with figure 4, also at 1200 CST, makes it clear that the sea breeze originates near the coastal area.

d) Since the return flow of this sea breeze is clearly shown in the figure, the averge height of the top of the sea breeze, that is, the turning point from sea breeze to its return flow, is found to be approximately 2,200 ft, which is about the same as that of the land breeze. The height of the top of the return flow varies more with time and, in some cases, extends to 9,000 ft (see near 1800 CST). The average speeds of the sea breeze and its return flow are approximately 5 and 6 mi hr^{-1}, respectively. Since the sea breeze and its return flow vary in height and speed as a function of time, the averaged value is given only a general magnitude. As the day proceeds, the height of the top of the return flow increases; it reaches its maximum altitude when the sea breeze is fully developed, then decreases at night, and finally disappears as the land breeze starts to blow. This cycle is clearly shown in figures 7a through 7c. Note that the stronger and deeper return flow of this sea breeze between 1740 and 1945 CST in figure 7 may be enhanced by the northeasterly prevailing synoptic flow, as mentioned previously.

e) The convergence line is observed. The data shown at the top of figure 7b are for station 20 located approximately 24 mi inland. From 1543 to 1618 CST, this station observed an average 3 mi hr^{-1} offshore wind component below 3,600 ft. The return flow of this offshore component, that is, onshore component, is also clearly shown. On the other hand, station STO at this time observed the sea breeze and its return flow. Thus, there exists a low-level convergence and an upper level divergence phenomenon located between those two stations and about 20 mi inland. This is supported by the data shown at 1708 and 1732 CST at station 21, since the maximum sea-breeze speed of this station is only 2 mi hr^{-1} at 1708 CST compared to 8 mi hr^{-1} at 1700 CST at STO. From the mesoscale analysis of the upper Texas coast surface temperature field, Hsu (1967) has suggested that the sea-breeze convergence appears to be located about 20 mi inland between the suggested cool pool and the northern warm belt in our study area. Furthermore, from the three-dimensional numerical study of the Texas coast sea breeze, McPherson (1968) predicts from his mathematical model that the most intense convergence and upward motion develop approximately 32 km inland, which is about 20 mi from shore.

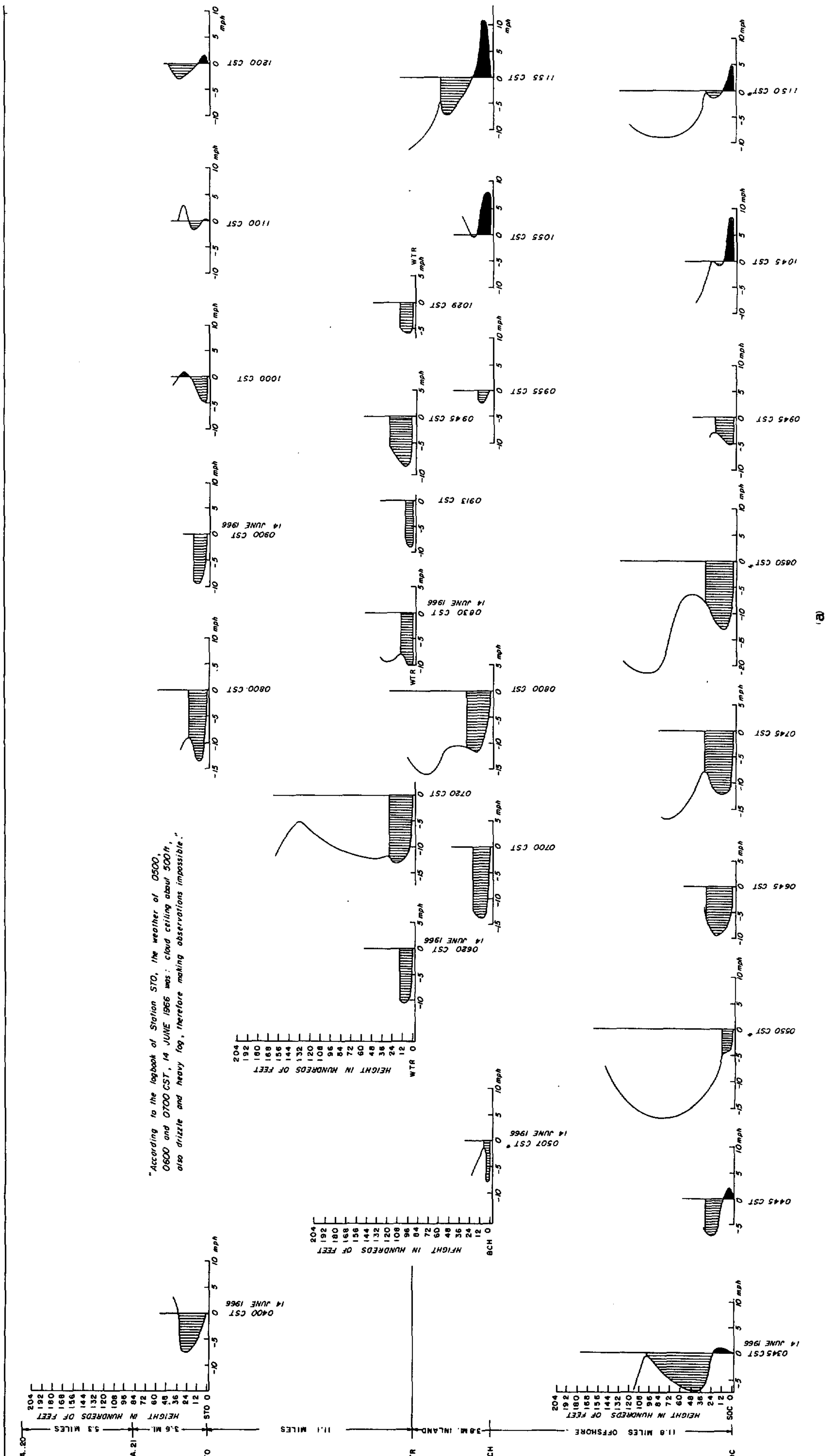

FIGURE 7.—Complete life cycle of the Texas coast land- and sea-breeze systems from (a) 0345 to 1200 CST on June 14, 1966; (b) 1245 to 2100 CST on June 14, 1966; and (c) 2150 CST on June 14 to 0640 CST on June 15, 1966.

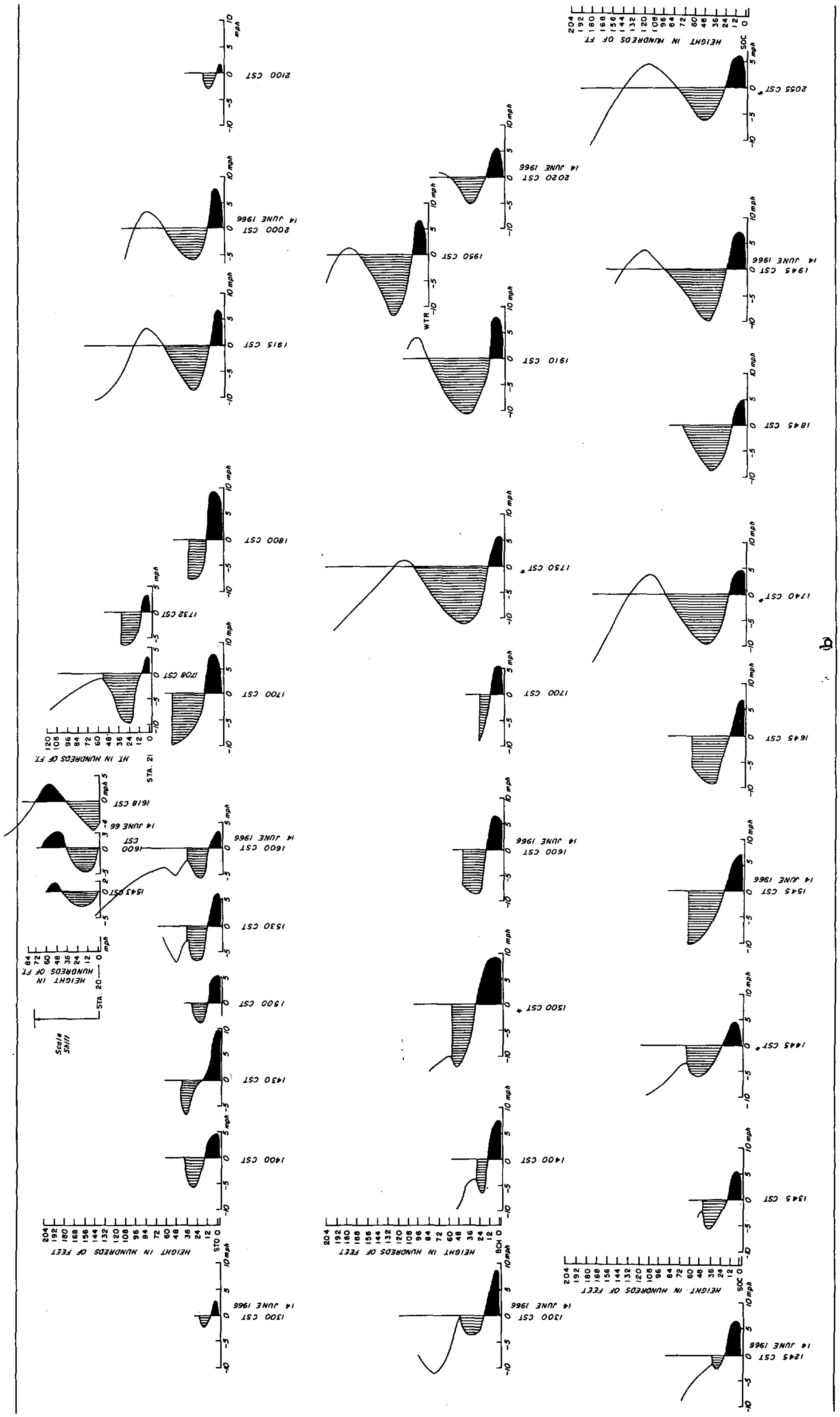

(b)

FIGURE 7.—Continued.

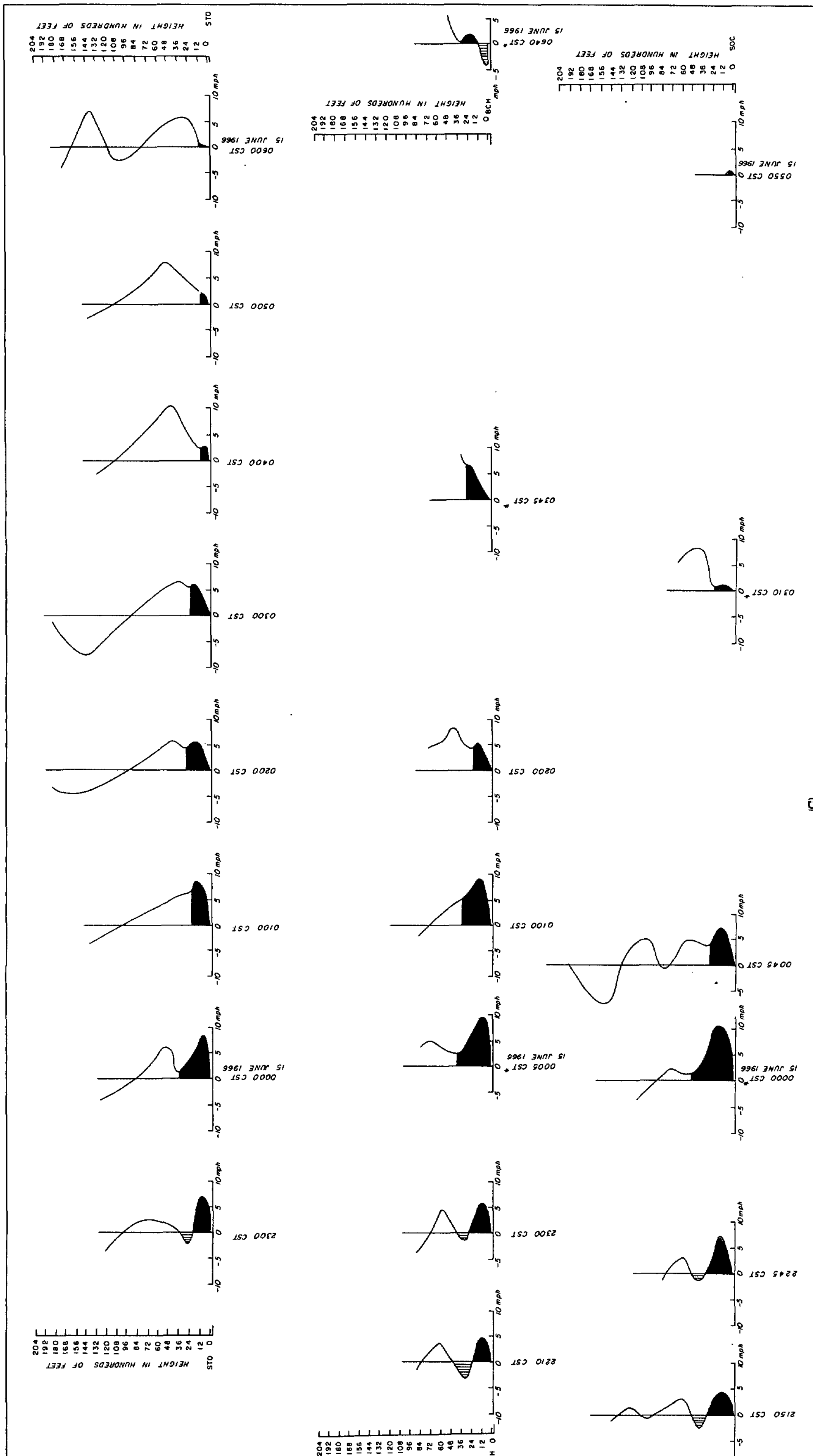

FIGURE 7.—Concluded.

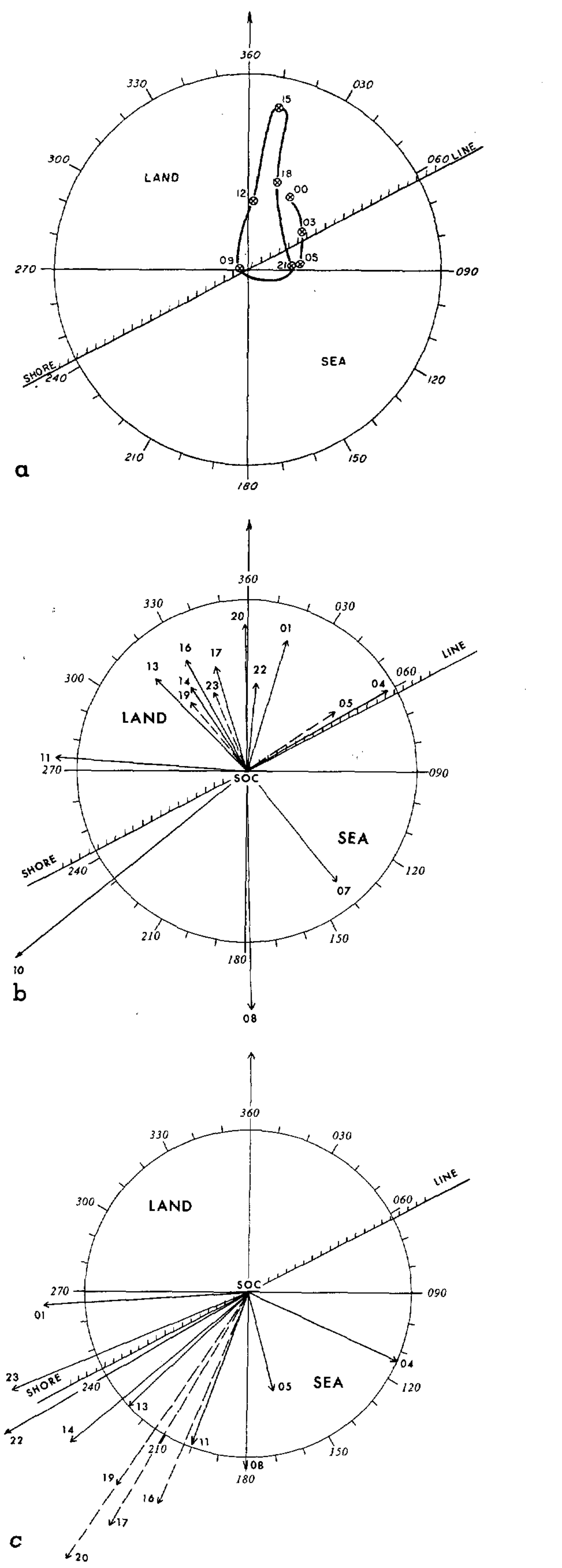

FIGURE 8.—(a) station BCH wind at the 500-ft level for June 15, 1965 (CST), after Eddy (1966); (b) station SOC wind at the 800-ft level for June 14, 1966 (CST); the distance from the center of the hodograph to the circle around the hodograph represents 10 mi hr^{-1}; and (c) same as (b), except station SOC wind at 4,500-ft level for June 14, 1966.

This convergence line is further supported by the evidence of cloud observation made at stations 20 and 21: at 1543 CST, a line of cumulus plus (Cu+) to the south and fractocumulus to the north of station 20; at 1618 CST, a line of developing Cu+ to the south and nondeveloped Cu to the north of station 20; at 1708 CST, Cu+ to the east, south, and west; and at 1732 CST, Cu+ to the southwest, south, and east, and also showers observed to the south and east (see "Sea Breeze Logbooks" by the Atmospheric Science Group 1965–1967). These same clouds were observed at STO. In fact, there was a rainbow to the east of STO at 1800 CST. At 1835 CST, it started raining (moderate shower) at STO; but this moderate shower ended at 1903 CST, according to the logbook for STO.

f) The mobile pibal unit was driven to WTR, after the observation of the convergence line was completed; to show that the pibal observations were good data; another pibal was released at 1950 CST. These data can be compared with those of other stations, say at 1910 CST at BCH; at 1945 CST at SOC; and at 1915 and 2000 CST at STO. They all show that the observers have the same capability. In other words, statistically speaking, the observed convergence data shown at station 20 is probably a real phenomenon.

Thus, figures 7a through 7c show a complete life cycle of the coastal air-circulation system. Furthermore, the low-level convergence and upper level divergence phenomenon is depicted from both observational and numerical results.

6. THE CORIOLIS EFFECT ON THE TEXAS COAST SEA BREEZE

The Coriolis effect on the veering of the sea breeze with time has been studied by Haurwitz (1947). Figure 8a shows an ellipse of the kind caused by this effect on the beach in our study area (Eddy 1966). Further evidence of the Coriolis effect on the Texas coast sea breeze is shown in figures 8b and 8c, which are the hodographs at 800 and 4,500 ft, respectively, over SOC on June 14, 1966. The arrows on the hodograph represent the wind at various times during the day and point toward the direction in which the wind is blowing. The distance from the center of the hodograph to the circle around the hodograph represents 10 mi hr^{-1}.

Starting from the first wind at 0400 CST in figure 8b, the wind veers continuously throughout the day and night; by 0100 CST on June 15, it has almost returned to parallel to the coast. Exceptions to this are given by the dashed arrows; they occur at the hours 0500, 1900, and 2300 CST.

At the 4,500-ft level (fig. 8c), there is a similar hodograph. With few exceptions, the wind veers with time at this level. However, the synoptic circulation is evident in this figure by the prevalence of northeasterly winds. As a result, the amount of veering is somewhat smaller than the lower levels.

From the observational results shown in figures 8a through 8c, it is clear that winds veer with time during the cycle under the effect of the Coriolis force over the upper Texas Gulf Coast. Further evidence on the Coriolis effect on the land- and sea-breeze system near the surface on the Gulf Coast may be found elsewhere (Hsu 1969*b*).

7. ALONGSHORE VARIATIONS OF THE TEXAS COAST SEA BREEZE

The alongshore variations of the sea breeze will be discussed in this section to give the total picture of the Texas coast sea breeze. A "parallel-to-the-coast" experiment was designed and performed during the summer of 1967 to study this alongshore variation on onshore and offshore wind components. Station BCH was selected as an arbitrary center point, and the experiment stretched 9.6 mi from BCH to HIS (toward Galveston) and to BZI (toward Louisiana). (See fig. 1 for the station location.) A series of pibal observations was then made at these three stations. The time interval between each pibal release was 30 min. The experiment was performed from 1200 on June 4 to 1230 CDT on June 5, 1967. Because of limited manpower, three 5-hr observational periods were chosen; namely, from 1200 to 1600; 2000 to 2400; and 0400 to 0800 CDT at BZI and HIS. At BCH, in addition to this, four observations from 1100 to 1230 CDT were made. The result of this experiment is shown in figures 9a through 9c. Note that station BZI was located near Clam Lake and other lakes in the eastern end of the study area, that HIS is near eastern Galveston Bay, and that BCH has no bay or lake nearby (fig. 1). These three stations were located just next to the shoreline of the gulf. Note that the convention in the figure is the same as that of figures 4 and 7.

Several general features can been seen from figures 9a through 9c:

a) Sea breeze starts earliest and strongest at HIS; it starts next at BCH and last at BZI in the afternoon and evening hours.

b) In the early morning hours, the sea breeze starts earliest and strongest at BZI, then at HIS, and last at BCH.

c) During the nighttime, the land breeze starts earliest and strongest at BCH, then at HIS, and last at BZI.

d) The effect of bay and lake on the low-level wind profile of the land breeze is pronounced.

Thus, owing to the presence of the shallow waters of bays and lakes along the upper Texas coast, alongshore variations on the land and sea breezes occur.

8. SYNTHESIZED MODEL OF THE COASTAL AIR-CIRCULATION SYSTEM

On the basis of the various field experiments mentioned previously, the observations are put together to give a synthesized empirical model of the coastal air-circulation system as a function of space and time. This system is shown in figures 10a through 10d for daytime and in figures 10e through 10h for nighttime phenomena, respectively. The model is shown graphically in such a way that:

a) The wind is decomposed into onshore flow and offshore flow. The lower portion of the onshore flow is the sea breeze, and that of the offshore flow is the land breeze.

b) The height or location of each arrow represents the position of the maximum speed (m sec^{-1}) of the land or sea breeze.

c) The elliptical shape in the figure represents the extent of the land- and sea-breeze circulation in the locality shown.

d) Since the convective condensation level is approximately at 900 mb, which is about 1 km, and since the 700-mb level (about 3 km) is near the top of the sea-breeze circulation according to the observations, these two isobaric surfaces as well as the surface level are labeled in the figure for reference.

e) The horizontal (x, y) plane in the figure shows schematically Galveston Bay and Sabine Lake, the orientation of the coastline, the land and sea areas, and the direction of true north.

We now explain briefly this coastal air-circulation system in sequence as shown in figures 10a through 10h. For a more detailed explanation, see Hsu (1969*a*). Let us start at 9 o'clock in the morning (local time 0900 hr in fig. 10a).

a) At this time, the air temperature over land is still cooler than that over the sea and adjacent waters. Thus, a baroclinic field prevails, and the land breeze is still blowing. Because of the effect of warmer bays and lakes, the land breeze on both ends is weaker than that near the central portion in the coastal area, but the land breeze on the right end is relatively stronger than that on the left end if one faces the onshore direction. Since there is a relatively strong land breeze near the central portion of the coast between Sabine Lake and Galveston Bay, the return flow over the region 20 km offshore may still produce scattered cumuli at this time, as shown schematically in the figure.

b) By noon (1200 hr), the land as a whole is warmer than the surrounding waters. A baroclinic field exists, resulting in a direct solenoidal circulation from near shore to about 20 km inland. However, the land breeze still prevails at this time at 20 km inland. Thus, low-level convergence is established. Scattered cumuli with a base at about 1 km tend to form a line. This sea-breeze front passes over a station near the central portion of the coast between Sabine Lake and Galveston Bay near late morning. An average sequence of characteristic changes occurs at the surface with the passage of the front: temperature drops approximately 5°F; relative humidity first drops 7 percent, then rises 14 percent; and, most pronounced, surface wind direction changes clockwise from northerly to southerly, a total directional change of 180° within 1 hr.

c) At 3 o'clock in the afternoon (1500 hr), the sea breeze is in the fully developed stage, since the air temperature difference between land and water reaches the maximum near noon. Superadiabatic lapse rates appear near the surface on land. At this time, there is a definite chance of formation of cumulus clouds, and showers will reach the ground at 4 to 5 o'clock in the afternoon from 30 to 40 km inland. The convergence line is fully developed at this time also, and the orientation of this line is approximately parallel to the coastline. Because of velocity divergence and relatively dry air in the return flow of the sea breeze, there is a subsidence phenomenon near the coastal area.

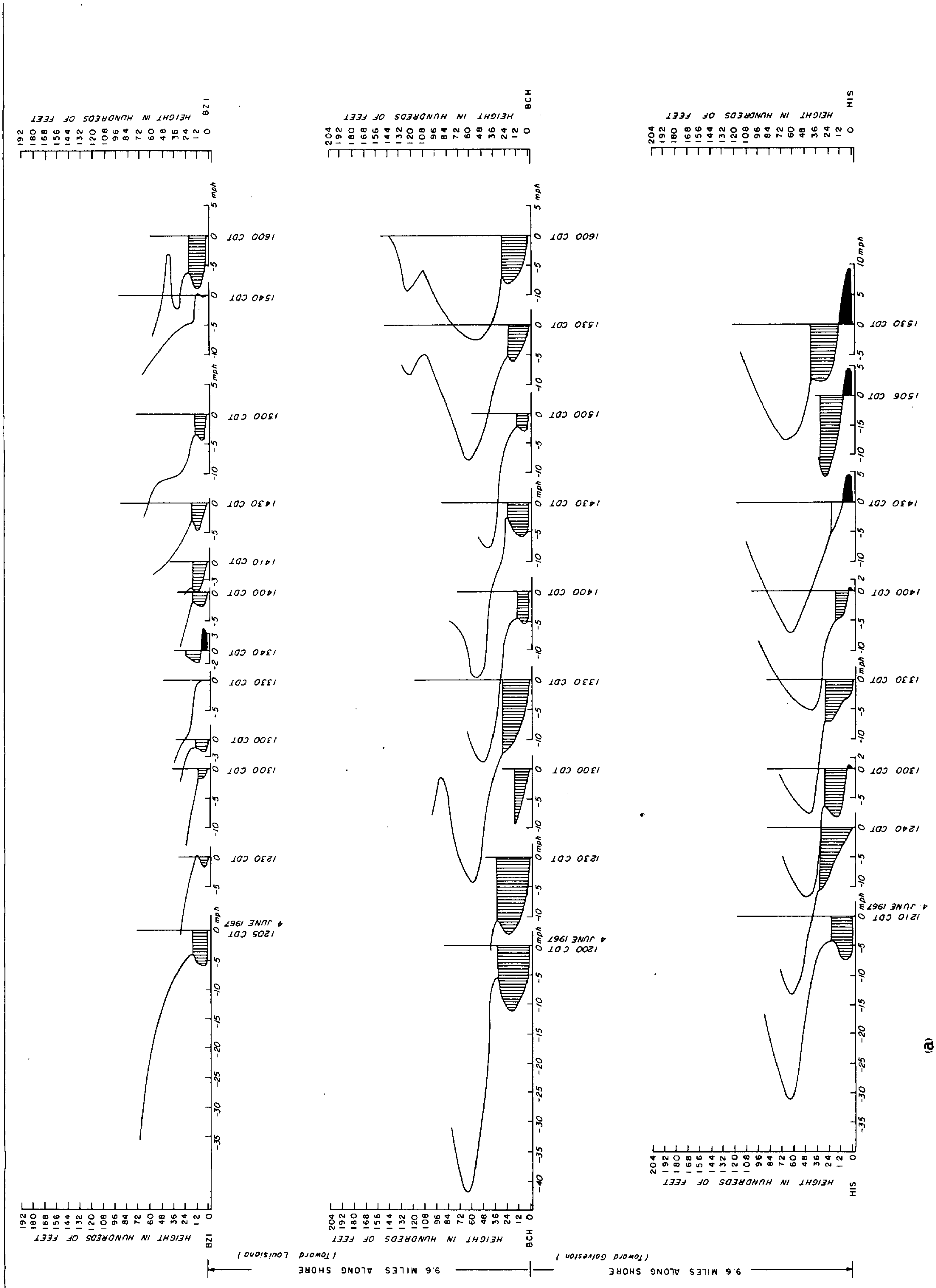

FIGURE 9.—The x-z-t three-dimensional variations of land and sea breezes at stations HIS, BCH, and BZI located along the coastline (convention is the same as that of figures 4 and 7); the time covered is from (a) 1200 to 1600 CDT on June 4, 1967; (b) 2000 to 2400 CDT on June 4, 1967; and (c) 0400 to 1230 CDT on June 5, 1967.

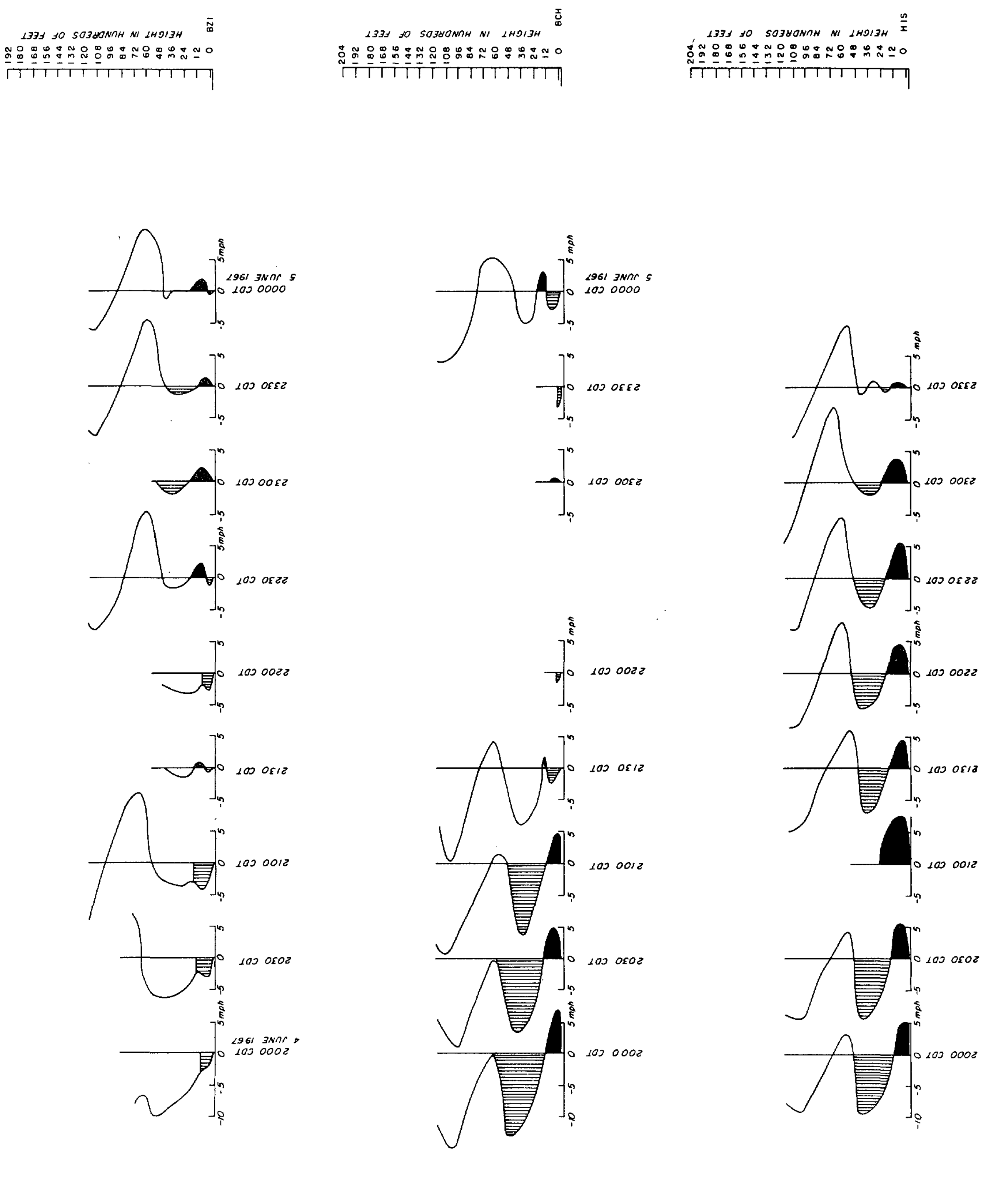

(b)

FIGURE 9.—Continued.

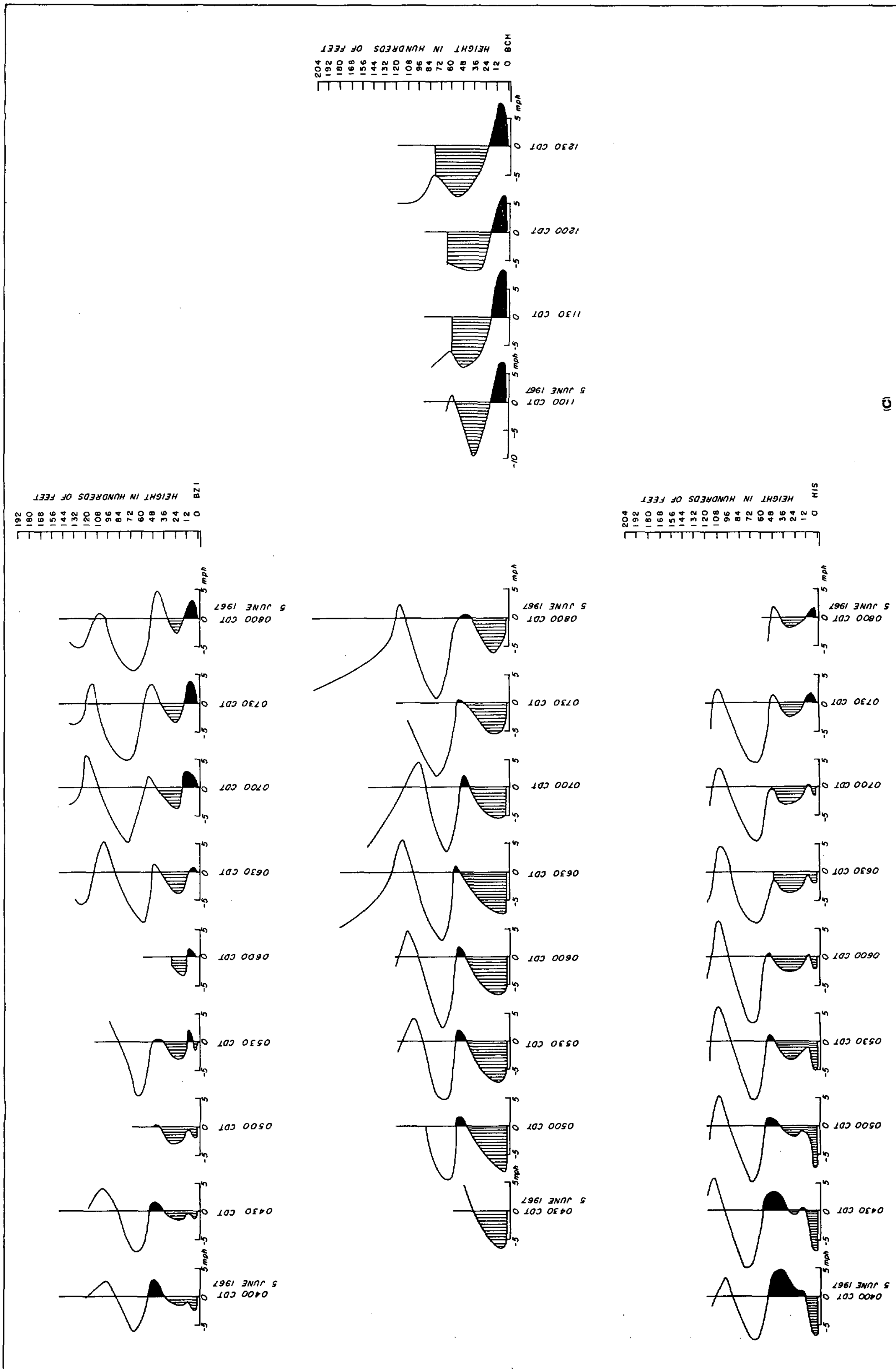

FIGURE 9.—Concluded.

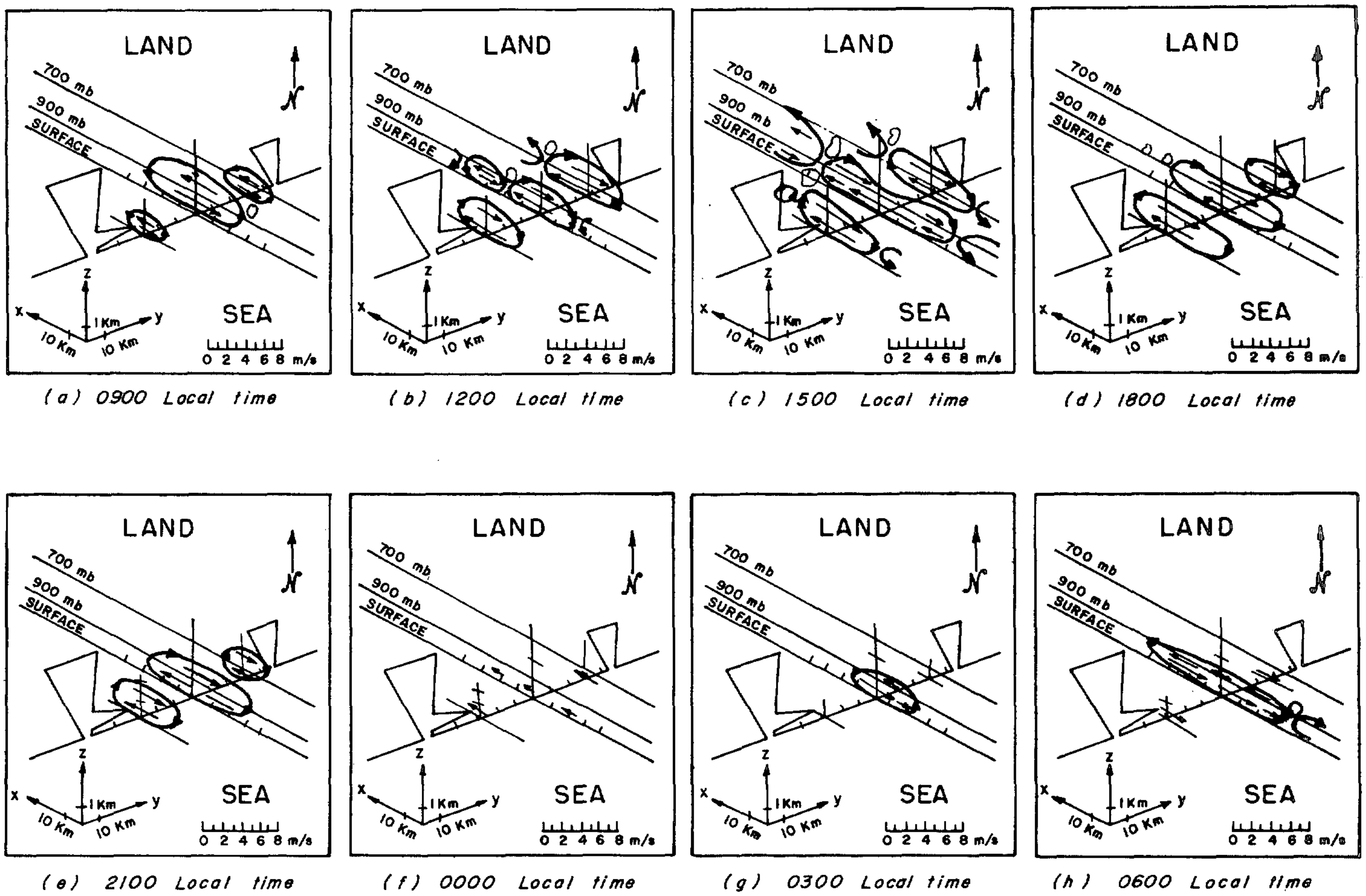

FIGURE 10.—Synthesized empirical model of the coastal air-circulation system.

d) About 6 o'clock in the afternoon (1800 hr), the land as a whole is still warmer than surrounding waters, but the baroclinic field is weaker than it was about 3 hr earlier. At this time, the sea breeze and its return flow are still prevailing. A few cumuli may still be lingering in the sky from 30 km and farther inland. Because the bay on the left is bigger than that on the right, the sea breeze at this time is stronger on the left end than on the right (if one faces the onshore direction).

e) At 9 o'clock in the evening (2100 hr, fig. 10e), the sun has set. At this time, the residual sea breeze and its return flow may be still prevailing, but the speed and strength are weaker than they were at 6 p.m., particularly near the surface.

f) Near midnight (2400 hr), the cool pool phenomenon caused by the effect of the sea breeze plus nocturnal cooling is about to form. The central portion of the pool is roughly parallel to the shoreline about 20 km inland. At this time, a temperature inversion and occasionally fog appear over land. A nearly barotropic field is prevailing over the area. The sea breeze at this time is almost gone. Surface wind is nearly calm on land.

g) About 3 o'clock in the morning (0300 hr), the cool pool is formed more completely. However, because the bays and lakes are warmer at this time, the horizontal temperature gradient from land to sea is larger near the central portion of the coast than at both ends in the area; thus, the land breeze will start earlier near the central portion of the coast. Since the cool pool is analogous to a cool "high" pressure region, a stable and barotropic situation will exist beyond 10 km inland. In the nearshore area, however, owing to the cool pool and the warmer sea water, a baroclinic field exists from the vicinity of the shoreline to 20 km offshore.

h) About 6 o'clock in the morning (0600 hr), the horizontal temperature gradient from land to sea is at its maximum. Thus, the land breeze will be stronger than at 0300 hr. A weak land-breeze convergence line associated with more scattered cumuliform clouds may be observed about 30 km offshore. The land breeze will continue to blow to the midmorning hours, and the sea-breeze cycle will start over again, as shown in figure 10a. Thus, the coastal air-circulation system has completed its life cycle.

9. COMPARISON BETWEEN THE SYNTHESIZED MODEL AND THE THREE-DIMENSIONAL NUMERICAL MODEL

The synthesized model discussed above is based on actual observations. A three-dimensional, time-dependent model of the Texas coast sea breeze has been obtained independently by McPherson (1968, chapter IV) by numerically integrating the equations of motion. We shall now compare these two models, that is, theoretical versus observational.

According to McPherson, the effect of irregularities in the coastline on the Texas coast sea breeze, specifically at Galveston Bay, is examined by means of a three-dimensional mathematical model that is essentially an extension of an earlier two-dimensional model developed by Estoque (1961, 1962). In the three-dimensional model, Galveston Bay is simulated by a square indentation of an otherwise straight coastline. The results of this model indicate that the presence of Galveston Bay creates a distortion in the sea-breeze convergence zone and an asymmetry in the vertical motion field associated with the zone. This asymmetric distribution of vertical motion around the bay is such that the greatest upward motion initially develops northwest of the bay and shifts later to northeast of the bay. In other words, the effect of the bay produces a landward distortion of the convergence zone, which forms onshore under the conditions of no prevailing synoptic scale flow, and this distortion is damped out with time as the convergence zone moves inland. Furthermore, the most intense convergence and upward motion develop in the northwest and northeast corners of the square model. By inference, these regions would therefore be preferred locations for convective showers. This intense convergence, and thus the maximum shower area, located in the northeast corner of Galveston Bay, have been verified by observations and shown in the synthesized model (fig. 10c).

The Coriolis effect on the sea-breeze cycle predicted by the mathematical model is verified by the observations. The dimensions and magnitude of the sea breeze and its return flow, including the mean speed, return point, and depth as a function of time, predicted by the numerical model are also verified by the observations.

Note that the above comparison statements have dealt with the sea-breeze part of the cycle only. The land-breeze part of the cycle synthesized by the observational results shown in figure 10 was not examined by the numerical model for the reason, according to McPherson, of a magnetic tape failure over an hour into the run. The integration resulted in only an 18-hr forecast, an unfortunate circumstance that eliminated the land-breeze part of the cycle. Nevertheless, the results of the sea-breeze part of the cycle were obtained and compare extremely well with the observational results presented here.

ACKNOWLEDGMENTS

I am grateful to Dr. Amos Eddy (presently with the Department of Meteorology at the University of Oklahoma) who provided guidance during the research. This paper was made possible by financial support from the National Science Foundation under Grant GA-376X to the University of Texas, Austin, and from the Geography Programs of the U.S. Navy Office of Naval Research (Contract N00014-69-A-0211-0003, Project No. NR 388 002) with the Coastal Studies Institute, Louisiana State University, and I gratefully acknowledge this assistance.

REFERENCES

Atmospheric Science Group, College of Engineering, The University of Texas, Austin, "Sea Breeze Logbooks," **1965-1967** (unpublished data).

Duchon, Claude E., "Techniques for Evaluating Meteorological Aircraft Data," *Technical Report* No. 9, Atmospheric Science Group, College of Engineering, The University of Texas, Austin, May **1968**, 93 pp.

Eddy, Amos, "The Texas Coast Sea-Breeze: A Pilot Study," *Weather*, Vol. 21, No. 5, May **1966**, pp. 162-170.

Eddy, Amos, and Hsu, Shih-Ang, "Statistical Evaluation of Surface Wind Strip Chart Data," *Technical Report* No. 12, Atmospheric Science Group, College of Engineering, The University of Texas, Austin, May **1968**, 52 pp.

Estoque, Mariano A., "A Theoretical Investigation of the Sea Breeze," *Quarterly Journal of the Royal Meteorological Society*, Vol. 87, No. 372, Apr. **1961**, pp. 136-146.

Estoque, Mariano A., "The Sea Breeze as a Function of the Prevailing Synoptic Situation," *Journal of the Atmospheric Sciences*, Vol. 19, No. 3, May **1962**, pp. 244-250.

Fisher, Edwin L., "An Observational Study of the Sea Breeze," *Journal of Meteorology*, Vol. 17, No. 6, Dec. **1960**, pp. 645-660.

Haurwitz, Bernhard, "Comments on the Sea-Breeze Circulation," *Journal of Meteorology*, Vol. 4, No. 1, Feb. **1947**, pp. 1-8.

Hess, Seymour L., *Introduction to Theoretical Meteorology*, Henry Holt and Co., New York, **1959**, 362 pp.

Hsu, Shih-Ang, "Mesoscale Surface Temperature Characteristics of the Texas Coast Sea Breeze," *Technical Report* No. 6, Atmospheric Science Group, College of Engineering, The University of Texas, Austin, May **1967**, 74 pp.

Hsu, Shih-Ang, "Objective Radiosonde Data Acquisition, Reduction, and Evaluation," *Technical Report* No. 13, Atmospheric Science Group, College of Engineering, The University of Texas, Austin, May **1968**, 78 pp.

Hsu, Shih-Ang, "Mesoscale Structure of the Texas Coast Sea Breeze," *Technical Report* No. 16, Atmospheric Science Group, College of Engineering, The University of Texas, Austin, Jan. **1969***a*, 237 pp.

Hsu, Shih-Ang, "Land- and Sea-Breeze Fronts Near 50 Cm on the Gulf Coast," *Bulletin of the American Meteorological Society*, Vol. 50, No. 11, Nov. **1969***b*, pp. 880-882.

McPherson, Ronald D., "A Three-Dimension Numerical Study of the Texas Coast Sea Breeze," *Technical Report* No. 15, Atmospheric Science Group, College of Engineering, The University of Texas, Austin, Aug. **1968**, 252 pp.

Moroz, William J., "A Lake Breeze on the Eastern Shore of Lake Michigan: Observations and Model," *Journal of the Atmospheric Sciences*, Vol. 24, No. 4, July **1967**, pp. 337-355.

[*Received September 23, 1969; revised April 2, 1970*]